AD613287

STEP LOAD MOVING ON THE SURFACE OF A HALF-SPACE OF A LOCKING MATERIAL - SUBSEISMIC CASE

by

Hans H. Bleich
Paul Weidlinger, Consulting Engineer

TECHNICAL DOCUMENTARY REPORT NO. WL TDR-64-8

COPY 2 OF 3
HARD COPY $. 3 00
MICROFICHE $. 0.75
63P

Research and Technology Division
AIR FORCE WEAPONS LABORATORY
Air Force Systems Command
Kirtland Air Force Base
New Mexico

February 1965

DDC
RECEIVED
APR 9 1965
DDC-IRA E

ARCHIVE COPY

WL TDR-64-8

STEP LOAD MOVING ON THE SURFACE OF A HALF-SPACE OF A LOCKING MATERIAL - SUBSEISMIC CASE

by

Hans H. Bleich
Paul Weidlinger, Consulting Engineer

February 1965

FOREWORD

The research reported here was performed under Project 5710, Subtask 13.144, Program Element 7.60.06.01.5, by Paul Weidlinger, Consulting Engineer, 777 Third Avenue, New York, NY, 10017, under Contract AF 29(601)-6055, during the period July 1963 to January 1964. The report was submitted 19 January 1965. The Air Force project monitor was 1Lt Cornelius J. Higgins, AFWL (WLDC).

This report has been reviewed and is approved.

Cornelius J. Higgins
CORNELIUS J. HIGGINS
1Lt USAF
Project Officer

Thomas J. Lowry, Jr.
THOMAS J. LOWRY, JR.
Colonel USAF
Chief, Civil Engineering Branch

R. A. House
R. A. HOUSE
Colonel USAF
Chief, Development Division

ABSTRACT

Considering a locking material prior to compaction as a special case of a nonlinearly hardening elastic material, conditions at a discontinuity--a locking front--are analyzed on the basis of three dimensional theory. This study leads to the important result that the major compressive principal stress at a locking front must always be normal to the front, even if the front is not plane. Based on this general result, the effect of a uniform step pressure traveling with subseismic velocity on the surface of a half-space is obtained for the case of a locking material which after compaction has elastic-Coulomb behavior. Such a material acts linearly elastic if the state of stress does not overcome internal friction, but slip occurs if the stresses reach a critical state defined by Coulomb friction. As a special case the solution applies also for a material which is linearly elastic after compaction. The stress, velocity and acceleration histories due to the traveling step pressure are discussed and compared to those in the one dimensional case of a suddenly applied uniform surface pressure.

This page intentionally left blank.

CONTENTS

Page

I Introduction. 1

II Three Dimensional Consideration of Locking Fronts 2

a) Non-Linear Elastic Materials 3

b) Locking Materials, Linearly Elastic after Compaction 12

c) Locking Materials, Linearly Elastic but Subject to Slip after Compaction. 15

III Effect of a Progressing Step Load on the Surface of a Half-Space. 20

Case A. The Material is Elastic after Locking 20

Case B. After Locking, the Material is Elastic, but Subject to Slip 24

IV Discussicn of Results 37

Typical Example. 39

V Summary of Conclusions. 42

Figures. 44

References 53

Distribution 54

LIST OF SYMBOLS

a	Acceleration.
c_p , c_s	Velocities of P- and S-waves in an elastic medium.
C, D	Constants of integration.
E	Young's modulus.
$f(\varphi)$	Function of φ.
$F(I_1)$	Function of I_1 .
I_1 , I_2 , I_3	Invariants of strain tensor.
k	Number defining behavior of locking materials, $0 < k < 1$.
$\bar{k} = \sigma_2/\sigma_1$	
L	Superscript in σ^L, indicating value at locking.
N	In Section II: a positive number.
N	In Section III: constant of integration.
p	Intensity of step load on surface.
r	Radius in polar system of coordinates r, φ.
$s > 0$	Quantity defining cohesion.
S	Superscript in ϵ^S , indicating: due to slip.
t	Time.
T	Superscript in ϵ^T , indicating: total.
u, u_x , u_y , u_L	Particle velocity, its x- and y-components, and value directly behind locking front, respectively.
U	Propagation velocity of a shock front, or of a locking front.
V	Velocity of propagation of surface pressure.
W	Strain energy function.
β	Inclination of locking front with respect to surface.
γ_{xy}	Shear strain.
$\gamma = \gamma(\varphi)$	Angle defining direction of principal stress σ_1 , Fig. 15.

$\Delta\sigma_{ij}$, $\Delta\epsilon_{ij}$	Increments of σ_{ij} , ϵ_{ij} .
ϵ	Locking strain (positive if compression).
ϵ_{ij} , ϵ_1 , ϵ_2	Strains and principal strains, respectively (positive if tensile).
φ	Angle in system of polar coordinates r, φ.
λ, μ	Lamé's constants.
$\lambda_0 > 0$, $\mu_0 > 0$	Constants.
ν	Poisson's ratio.
ρ	Density.
$\sigma > 0$	Defined by Eq. (2-41).
σ_{ij} , σ_1 , σ_2	Stresses and principal stresses, respectively (positive if tensile).
τ	Shear stress.

This page intentionally left blank.

I INTRODUCTION

A preceding report*[1], considers the effect of a step pressure progressing with velocity V on the surface of a half-space, Fig. 1, when the behavior of the material is governed by internal Coulomb friction. The investigation [1] studies steady-state solutions, assuming that the material acts linearly elastic if the state of stress does not overcome internal friction, but slip occurs if the stresses reach a critical state defined by internal Coulomb friction. Approximations made in the analysis permit closed solutions, but restrict the result to velocities V below a certain limit.

The present investigation concerns the equivalent steady-state problem, Fig. 2, for an ideal locking material which, after compaction (i.e., after locking) has the elastic-Coulomb properties assumed in [1]. As the first step in the analysis a study of the locking front is made. Considering the locking material prior to compaction as a special case of a nonlinearly elastic material, available three dimensional theory for nonlinearly elastic media is used to obtain a condition on the state of stress at a front of discontinuity in such a medium. Thereafter, the condition obtained at the front, and the approximate procedure developed in [1] for materials subject to Coulomb friction and slip are jointly applied, leading to results in closed form. The approximation restricts the results to velocities V which are less than a certain limit.

If the value of the internal friction is sufficiently large, slip will not occur, and the present analysis contains the solution for the problem shown in Fig. 2 for a locking material which acts linearly elastic after compaction. The problem of one dimensional wave propagation in such a material has been treated [2], but the two dimensional case, Fig. 2, has not been considered previously.

---

* Numbers in brackets refer to References on page 53.

II THREE DIMENSIONAL CONSIDERATION OF LOCKING FRONTS

The problem of determining the effect of a uniform pressure p(t) acting on the surface of a half-space, Fig. 3, involves only one dimensional strain, so that it is sufficient to know the stress-strain diagram relating σ_{xx} and ϵ_{xx}. For soils, when such diagram has the character of Fig. 4a, approximate results have been obtained by replacing the actual diagram by that of ideal locking materials, Fig. 4b or c, [3]. The simplification implies that all stresses vanish until the strain ϵ_{xx}, which in this case equals the volumetric strain, has reached a certain value defining the point of compaction.

In the case of one dimensional wave propagation, Fig. 3, symmetry requires that the stress at the plane locking front be normal to this front (i.e., there can be no shear stress). The velocity V of the front as a function of σ_{xx} can then be obtained from the Rankine-Hugoniot relations, using the stress-strain diagram, Fig. 4.

In more general problems in two or three dimensions a sufficiently small element of the locking front may still be considered plane, Fig. 5, but the argument of symmetry cannot be used to draw the conclusions that the resultant of the stress just behind the front is normal to the front and that the shear stress τ_N vanishes. Nevertheless, it will be shown below that the above conclusion is valid in the multidimensional case too, but the demonstration requires a much more involved reasoning.

a) Non-linear Elastic Materials

Postponing the complications due to the effect of slip in a Coulomb type material, this section is restricted to non-linear elastic materials which harden with reduction in volume. Conclusions drawn can then be applied to ideal locking materials, because they are special cases of such a non-linearity.

To study locking fronts, a mathematical description of three dimensional behavior is required for a homogeneous, non-linear material which acts in one dimensional strain according to Fig. 4a. Using the concept of a "strain-energy function" W, [4, p. 95], the stresses σ_{ij} in an elastic material may be obtained as derivatives of W with respect to the strains ϵ_{ij},

$$\sigma_{ii} = \frac{\partial W}{\partial \epsilon_{ii}} \quad , \quad \sigma_{ij} = \frac{\partial W}{2\partial \epsilon_{ij}} \tag{2-1}$$

where the subscripts i and j become, in turn the Cartesian coordinates x, y and z.* For isotropic materials the strain energy function must be invariant to transformation of the coordinates, which requires W to be a function of the invariants of the strain tensor. For linear elastic materials this leads [4, p. 102] to the function

---

* Note that [4] uses different symbols and a different definition of the shear strain. To obtain the equations in this paper the following substitutions were made: The stresses in [4], X_x, X_y, etc., become σ_{xx}, σ_{xy}, etc., respectively; longitudinal strains e_{xx}, e_{yy}, e_{zz} become ϵ_{xx}, ϵ_{yy}, ϵ_{zz}, while the shear strains e_{xy}, e_{yz}, e_{zx} become $2\epsilon_{xy}$, $2\epsilon_{yz}$, and $2\epsilon_{zx}$. As a result of the change in definition of the shear strains, the quantities ϵ_{ij} are components of a tensor.

$$W = \frac{\lambda+2\mu}{2} (I_1)^2 - 2\mu I_2 \tag{2-2}$$

where λ and μ are constants, while

$$\begin{aligned} I_1 &= \epsilon_{xx} + \epsilon_{yy} + \epsilon_{zz} \\ I_2 &= \epsilon_{yy}\,\epsilon_{zz} + \epsilon_{zz}\,\epsilon_{xx} + \epsilon_{xx}\,\epsilon_{yy} - \epsilon_{xy}^2 - \epsilon_{yz}^2 - \epsilon_{zx}^2 \end{aligned} \tag{2-3}$$

I_1 and I_2 are invariants of the strain tensor. It is noted that I_1 describes the change in volume of an element.

To describe the most general case of an isotropic non-linear material, the constants λ and μ in Eq. (2-2) should be considered as functions of all invariants of the strain, of which there are three. In addition to I_1 and I_2, given by Eqs. (2-3), there is a third one [5, p. 180, Eq. (25.11)]

$$\begin{aligned} I_3 = {} & \epsilon_{xx}\,\epsilon_{yy}\,\epsilon_{zz} + 2\epsilon_{xy}\,\epsilon_{yz}\,\epsilon_{zx} - \epsilon_{xx}\,\epsilon_{yz}^2 - \\ & - \epsilon_{yy}\,\epsilon_{xz}^2 - \epsilon_{zz}\,\epsilon_{xy}^2 \end{aligned} \tag{2-3a}$$

However, in order to describe a material which becomes harder with consolidation, i.e., with volume change, λ and μ should be just functions of I_1, which defines the volumetric strain. It will be shown below that for the present purpose, one may assume that λ and μ are proportional,

$$\lambda = \lambda_o F(I_1)$$

$$\mu = \mu_o F(I_1) \tag{2-4}$$

where λ_o and μ_o are positive values having the dimensions of Lamé's constants λ and μ, and the function $F(I_1)$ is always positive. In order to represent a hardening material, the derivative of F must satisfy the inequality

$$\frac{dF}{dI_1} \leq 0 \tag{2-5}$$

when $I_1 < 0$. Substitution of Eqs. (2-4) into (2-2) gives

$$W = \frac{\lambda_o + 2\mu_o}{2} F(I_1)\, I_1^{\,2} - 2\mu_o F(I_1)\, I_2 \tag{2-6}$$

Application of Eqs. (2-1) furnishes, after rearrangement, the stress-strain relations

$$\sigma_{ii} = F(I_1)(\lambda_o I_1 + 2\mu_o \epsilon_{ii}) + \frac{1}{2} F'(I_1)[(\lambda_o + 2\mu_o) I_1^{\,2} - 4\mu_o I_2] \tag{2-7}$$

and for $i \neq j$

$$\sigma_{ij} = 2F(I_1)\, \mu_o\, \epsilon_{ij} \tag{2-8}$$

where

$$F'(I_1) = \frac{dF(I_1)}{dI_1} \tag{2-9}$$

To demonstrate that the assumption made in writing Eqs. (2-4) is permissible, it will be shown that it leads to a diagram of the type of Fig. 4 in the case of uni-axial strain in the direction of the x-axis when all values ϵ_{ij} vanish except ϵ_{xx}. For this case Eqs. (2-3) give $I_1 = \epsilon_{xx}$ and $I_2 = 0$, such that $F(I_1) = F(\epsilon_{xx})$, $F'(I_1) = F'(\epsilon_{xx})$. The stress-strain relation is obtained by substituting these expressions into Eq. (2-7) for i = x:

$$\sigma_{xx} = (\lambda_o + 2\mu_o)[\epsilon_{xx} F(\epsilon_{xx}) + \frac{1}{2} \epsilon_{xx}^2 F'(\epsilon_{xx})] \qquad (2\text{-}10)$$

By definition, the function F is positive and by virtue of Eq. (2-5) F increases for negative (compressive) strains with $|\epsilon_{xx}|$. The term $\epsilon_{xx} F(\epsilon_{xx})$ in Eq. (2-10) has therefore the character of Fig. 4a, including the negative sign in the range $\epsilon_{xx} < 0$. The other term, $\frac{1}{2} \epsilon_{xx}^2 F'(\epsilon_{xx})$ is also negative. To assure that its absolute value also increases similarly, we prescribe

$$F''(\epsilon_{xx}) > 0 \qquad (2\text{-}11)$$

Both terms having the character of Fig. 4a, the entire expression will have the same character. The strain-energy function (2-6) furnishes therefore a three dimensional expression for materials having a one dimensional stress-strain diagram of the type of Fig. 4, provided the function F satisfies Eqs. (2-5) and (11). [An example of a function satisfying the requirements is $F = \exp(-N\epsilon_{xx})$, where N is a positive number. It is easily verified that Eq. (2-10) gives

a σ-ϵ diagram of the type of Fig. 4a.)

The stress-strain relation (2-1) and the expression (2-6) for W can now be introduced into the Rankine-Hugoniot relations. Consider two dimensional wave propagation for the case of plane strain. Let the x and y axes, respectively, be normal and tangential to the front, Fig. 6, while the z-axis is normal to the plane of the paper.

Fig. 6 indicates a rectangular, infinitesimally small element, in its original shape ABCD, and in its distorted shape A'B'CD, after the wave front has passed over it. Let U be the propagation velocity of the front. In the time dt the wave front has traveled the distance U dt = $\overline{AD}$, while point A has traveled to A', the x and y components of its motion being $u_x dt$ and $u_y dt$, respectively, where u_x , u_y are the components of the particle velocities. From Fig. 6 one may read directly the longitudinal strain

$$\epsilon_{xx} = - \frac{u_x}{U} \tag{2-12}$$

The minus sign is due to the fact that the positive directions of σ_{xx} and u_x are opposite each other. Noting further that the conventional shear strain γ_{xy} equals $2\epsilon_{xy}$, one finds similarly

$$\gamma_{xy} = 2\epsilon_{xy} = - \frac{u_y}{U} \tag{2-13}$$

In the limit dt $\rightarrow$ 0 the distance AB equals A'B' such that on the shock front $\epsilon_{yy} = 0$. Further, because of plane strain, $\epsilon_{xz} = \epsilon_{yz} = \epsilon_{zz} = 0$

such that only ϵ_{xx} and ϵ_{xy} need be considered further. Eqs. (2-3) become therefore

$$I_1 = \epsilon_{xx}$$
$$I_2 = - \epsilon_{xy}^2 \tag{2-14}$$

and from Eq. (2-7):

$$\sigma_{xx} = (\lambda_o + 2\mu_o)\, \epsilon_{xx}\, F(\epsilon_{xx}) + \frac{1}{2}\, [(\lambda_o + 2\mu_o)\, \epsilon_{xx}^2 + 4\mu_o\, \epsilon_{xy}^2]\, F'(\epsilon_{xx}) \tag{2-15}$$

$$\sigma_{yy} = \sigma_{zz} = \lambda_o\, \epsilon_{xx}\, F(\epsilon_{xx}) + \frac{1}{2}\, [(\lambda_o + 2\mu_o)\, \epsilon_{xx}^2 + 4\mu_o\, \epsilon_{xy}^2]\, F'(\epsilon_{xx}) \tag{2-16}$$

The shear stresses are obtained from Eq. (2-8):

$$\sigma_{xy} = 2\mu_o\, \epsilon_{xy}\, F(\epsilon_{xx}) \tag{2-17}$$

$$\sigma_{xz} = \sigma_{yz} = 0 \tag{2-18}$$

In the time dt in which the front engulfs the element ABCD, Fig. 6, the x and y-components of the velocities of all the particles in the element are changed by u_x and u_y, respectively. The mass of the element being $\rho\, U\, dt\, dy\, dz$, the change in momentum in the x-direction can be expressed by the stress σ_{xx},

$$\rho\, U\, u_x = - \sigma_{xx} \tag{2-19}$$

where ρ is the density. A similar relation applies for the y-direction

$$\rho \; U \; u_y = - \; \sigma_{xy} \tag{2-20}$$

The minus signs appear again because the directions of the stresses shown in Fig. 6 are opposite to the positive directions of the velocities. Substituting the values of u_x and u_y into Eqs. (2-12, 13), one finds

$$\sigma_{xx} = \rho \; U^2 \; \epsilon_{xx} \tag{2-21}$$

$$\sigma_{xy} = 2\rho \; U^2 \; \epsilon_{xy} \tag{2-22}$$

Eqs. (2-21) and (2-15) give

$$\rho \; U^2 = (\lambda_o + 2\mu_o) \; F(\epsilon_{xx}) + \frac{1}{2} \left[(\lambda_o + 2\mu_o) \; \epsilon_{xx}^2 + 4\mu_o \; \epsilon_{xy}^2 \right] \frac{F'(\epsilon_{xx})}{\epsilon_{xx}} \tag{2-23}$$

The division by ϵ_{xx}, required to obtain this result, is always permitted, because a consolidation front is being investigated, such that $\epsilon_{xx} \neq 0$. Substituting Eq. (2-22) into (2-17) gives, after division by $2\epsilon_{xy}$, the alternative relation

$$\rho \; U^2 = \mu_o \; F(\epsilon_{xx}) \tag{2-24}$$

This equation applies only if $\epsilon_{xy} \neq 0$, the division not being possi-

ble if $\epsilon_{xy} = 0$.

If the shear strain ϵ_{xy} does not vanish, Eqs. (2-23, 24) should both be valid; however, it can be shown easily that this is not the case. Noting Eq. (2-5) and $\epsilon_{xx} < 0$, $\lambda_o > 0$, $\mu_o > 0$, both terms on the right hand side of Eq. (2-23) are positive, such that

$$\rho\ U^2 > (\lambda_o + 2\mu_o)\ F(\epsilon_{xx}) \tag{2-25}$$

This is incompatible with Eq. (2-24). The contradiction disappears only if $\epsilon_{xy} = 0$. In this case Eqs. (2-22 and 20) give

$$\sigma_{xy} = 0 \quad , \quad u_y = 0 \tag{2-26}$$

It is therefore concluded that <u>on a compaction front the stress resultant and the particle velocity are normal to the front</u>.

Introduction of $\epsilon_{xy} = 0$ into Eqs. (2-15, 16) gives the following expressions for the stresses at the front:

$$\sigma_{xx} = (\lambda_o + 2\mu_o)\ \epsilon_{xx}\ F(\epsilon_{xx}) + \frac{\lambda_o + 2\mu_o}{2}\ \epsilon_{xx}^2\ F'(\epsilon_{xx}) \tag{2-27}$$

$$\sigma_{yy} = \sigma_{zz} = \lambda_o\ \epsilon_{xx}\ F(\epsilon_{xx}) + \frac{\lambda_o + 2\mu_o}{2}\ \epsilon_{xx}^2\ F'(\epsilon_{xx}) \tag{2-28}$$

λ_o, μ_o and F being by definition positive, while $\epsilon_{xx} < 0$ (compaction) and $F' < 0$ [see Eq. (2-5)], all terms on the right-hand side of Eqs. (2-27, 28) are necessarily negative. Using these facts,

the relative magnitudes of σ_{xx} and $\sigma_{yy} = \sigma_{zz}$ may be compared. The expressions for these stresses differ only in the term containing $F(\epsilon_{xx})$, and one finds the inequality

$$|\sigma_{xx}| \geq |\sigma_{yy}| = |\sigma_{zz}| \tag{2-29}$$

b) Locking Materials, Linearily Elastic after Compaction

The results of Section a) will now be applied to an ideal locking material having a uni-axial stress-strain diagram of the type Fig. 4c, i.e. a material which becomes linearily elastic after locking. Using a limiting process, the diagram 4c is being considered as a special case of the diagram in Fig. 7, in the limit $\sigma_{xx}^{L} \rightarrow 0$. The material corresponding to Fig. 7 is defined as follows:

For compressive strains between 0 and $-\epsilon$, the stresses are obtained from the non-linear relations (2-27, 28), reaching values σ_{xx}^{L} and $\sigma_{yy}^{L} = \sigma_{zz}^{L}$ for $\epsilon_{xx} = -\epsilon$. For strains beyond this limit the material is deemed to be linear, having material constants E and ν. The stress increments $\Delta\sigma_{ii}$ after locking,

$$\Delta\sigma_{ii} = \sigma_{ii} - \sigma_{ii}^{L} \tag{2-30}$$

can be obtained from the strain increments $\Delta\epsilon_{ii}$ beyond the locking strain by using the conventional elastic relations. The x-component of the strain change is

$$\Delta\epsilon_{xx} = \epsilon_{xx} + \epsilon \tag{2-31}$$

All other components of the strain ϵ_{ij} vanish at the front, Eqs. (2-13a, 13b, 26a), such that all increments $\Delta\epsilon_{ij}$ also vanish, except $\Delta\epsilon_{xx}$. In this situation (transverse strains being inhibited), the ratio of the transverse and longitudinal stresses according to linear theory of elasticity is $\frac{\nu}{1-\nu}$, such that

$$\Delta\sigma_{yy} = \Delta\sigma_{zz} = \frac{\nu}{1-\nu}\Delta\sigma_{xx} \tag{2-32}$$

Consider now Eq. (2-30) in the limit

$$\lim \sigma_{xx}^{L} \rightarrow 0 \tag{2-33}$$

Because the inequality (2-29) requires the absolute values of σ_{yy} and σ_{zz} to be less than $|\sigma_{xx}|$, it is necessary that

$$\lim \sigma_{yy}^{L} = \lim \sigma_{zz}^{L} \rightarrow 0 \tag{2-33b}$$

Going to the limit $\sigma_{ii}^{L} \rightarrow 0$, Eq. (2-30) becomes therefore

$$\sigma_{ii} = \Delta\sigma_{ii} \tag{2-34}$$

and substitution into Eq. (2-32) leads to a relation for the stresses just behind the consolidation front

$$\sigma_{yy} = \sigma_{zz} = \frac{\nu}{1-\nu}\sigma_{xx} \tag{2-35}$$

while according to Section a) all shear stresses vanish:

$$\sigma_{xy} = \sigma_{yz} = \sigma_{zx} = 0 \tag{2-35a}$$

These relations apply immediately behind the compaction front, and will be used in Section III as boundary conditions when determining

the stresses after compaction at points anywhere behind the front.

The value of the increment of the strain $\Delta\epsilon_{xx}$ in terms of $\Delta\sigma_{xx}$ obtained from the conventional elastic relations is

$$\Delta\epsilon_{xx} = \frac{1-\nu-2\nu^2}{E(1-\nu)}\,\Delta\sigma_{xx} \tag{2-36}$$

or from Eqs. (2-31) and (2-34)

$$\epsilon_{xx} = -\,\epsilon + \frac{1-\nu-2\nu^2}{E(1-\nu)}\,\sigma_{xx} \tag{2-37}$$

This relation applies for the stress-strain diagram Fig. 4c. To obtain the relation corresponding to Fig. 4b, let $E \to \infty$, with the result

$$\epsilon_{xx} = -\,\epsilon \tag{2-38}$$

This equation defines the strain immediately behind the compaction front. Substituting this value into Eq. (2-21) gives the velocity U of the front

$$U = \sqrt{\frac{-\,\sigma_{xx}}{\rho\epsilon}} \tag{2-39}$$

Due to $\sigma_{xx} < 0$ (compression), the expression under the root is positive, as it should be. (Note that only the positive value of the square root has physical meaning.)

c) Locking Materials, Linearly Elastic but Subject to Slip after Compaction

Consider finally locking fronts in two dimensional problems of plane strain for an ideal locking material which behaves linearly elastic provided internal friction of the Coulomb type is not overcome, but which will slip when the stresses satisfy Coulomb's rule.

Ref. [1, p. 6, 7] contains for this case a formulation of the slip condition which is convenient for the present study of the state of stress at the compaction front. Let σ_1, σ_2 be the major and minor principal stresses in the plane of action, both being restricted to compression, such that

$$\sigma_1 < 0 \quad , \quad \sigma_2 < 0 \quad , \quad -\sigma_1 \geq -\sigma_2 \tag{2-40}$$

Defining a quantity σ by the relation

$$\sigma = -(\sigma_1 + s) \tag{2-41}$$

the possible states of stress in the material are further restricted to

$$-\sigma_2 \geq k\,\sigma \tag{2-42}$$

where k is a positive number, $k < 1$, which is related to the angle of interior friction, while $s > 0$ defines the value of cohesion. No slip can occur if

$$-\sigma_2 > k\,\sigma \tag{2-43}$$

while slip occurs if

$$-\sigma_2 = k\,\sigma \tag{2-44}$$

Values of $-\sigma_2 < k\,\sigma$ can, by definition, not occur in this material.

The above conditions involve only the principal stresses σ_1 and σ_2, in the plane of the two dimensional problem. In order that this formulation remains valid the third stress σ_3 must lie between the other two, $-\sigma_1 \geq -\sigma_3 \geq -\sigma_2$.

Concerning the strains, it was assumed in [1] that the plastic (or slip) deformations occur without volume change, while the elastic deformations are negligible. In the present case, a more refined definition must be derived, allowing for the elastic strains.

Retaining the result obtained in Section a), stating that the stress resultant at the compaction front is normal to this front, the state of stress and the associated strains can be obtained relatively simply. Consider a rectangular element ABCD, Fig. 8, as the compaction front passes over it, and let x be a coordinate at right angles to the front. On the front, the tangential strains must vanish such that the only non-vanishing strain is ϵ_{xx}^{T}, where the superscript T indicates total strain from all causes. For an elastic-plastic material this total strain is the sum of an elastic contribution (in the present case non-linear) and of the slip strain, and we have the relations

$$\epsilon_{xx} + \epsilon_{xx}^{S} = \epsilon_{xx}^{T}$$

$$\epsilon_{yy} + \epsilon_{yy}^{S} = \epsilon_{yy}^{T} \equiv 0 \qquad (2\text{-}45)$$

$$\epsilon_{zz} + \epsilon_{zz}^{S} = \epsilon_{zz}^{T} \equiv 0$$

where ϵ_{ii} are the elastic strains, ϵ_{ii}^{S} the slip strains, and y,z are coordinates in the plane of the front. Adding the three equations gives

$$\epsilon_{xx}^{T} = (\epsilon_{xx} + \epsilon_{yy} + \epsilon_{zz}) + (\epsilon_{xx}^{S} + \epsilon_{yy}^{S} + \epsilon_{zz}^{S}) \qquad (2\text{-}46)$$

The sum of the three strains ϵ_{ii} is the volumetric strain ϵ_v, and similarly the sum of the three strains ϵ_{ii}^{S} is the volume change during slip. In conformity with [1] the latter volume change vanishes, such that

$$\epsilon_{xx}^{T} = \epsilon_v \qquad (2\text{-}47)$$

The total strain ϵ_{xx}^{T} is therefore equal to the elastic volume change. For an ideal locking material, corresponding to Fig. 4b, the volume change does not depend on the stress level, $\epsilon_v = -\epsilon$, or

$$\epsilon_{xx}^{T} = -\epsilon \qquad (2\text{-}48)$$

where ϵ is the locking strain. Eq. (2-48) is identical with Eq. (2-38) and the velocity of the compaction front is again given by Eq. (2-39).

The state of stress in case of slip is of course different from the elastic case, Eq. (2-35). Using Eqs. (2-41 and 44), the major principal stress is $\sigma_1 \equiv \sigma_{xx}$, while $\sigma_2 = \sigma_{yy}$, and one finds the tangential stress

$$\sigma_{yy} = k(\sigma_{xx} + s) \tag{2-49}$$

If cohesion vanishes, s = o, and

$$\sigma_{yy} = k\ \sigma_{xx} \tag{2-50}$$

This value of the stress σ_{yy} applies immediately behind the compaction front, and will be used later as boundary condition when determining the stress field behind the front.

Eqs. (2-49) and (2-50) apply only if slip actually occurs, which depends on the relative values of k and ν. To decide if slip occurs, consider Eq. (2-35) for σ_{yy} without slip,

$$\sigma_{yy} = \frac{\nu}{1-\nu}\ \sigma_{xx} \tag{2-51}$$

If in the case without cohesion

$$\frac{\nu}{1-\nu} \leq k \tag{2-52}$$

Eq. (2-43) is not satisfied, such that slip must occur and Eq. (2-50) is to be used. If on the other hand

$$\frac{\nu}{1-\nu} > k \qquad (2\text{-}53)$$

Eq. (2-43) is satisfied such that the behavior a. the front is elastic and the elastic relation (2-35) applies.

III EFFECT OF A PROGRESSING STEP LOAD ON THE SURFACE OF A HALF-SPACE

The principal subject of this study is the case of locking materials which may slip after compaction. However, for purposes of presentation it is more convenient to consider first the less interesting case of a material which, after locking, acts elastically, without slip. The latter material is considered in this Section as Case A, while the material with slip is considered as Case B.

Case A. After Locking, the Material is Elastic.

Figure 9 indicates the progressing step load and a system of polar coordinates φ, r moving with the load. Dimensional considerations, similar to those used in [1], require that in the present problem the stresses be proportional to the load p, but otherwise solely functions of the variable φ,

$$\sigma, \tau \ldots = p\, f(\varphi) \; .$$

The fact that the stresses are only a function of φ implies that the locking front is a plane, inclined at an as yet unknown angle $\varphi = \beta$.

The state of stress in the wedge of angle β behind the front is governed by the appropriate equations of elasticity. In similarity to [1], the present analysis will be restricted to velocities V which are a fraction of the velocities c_p and c_s of wave propagation in the elastic material after locking. The differential equations for the stresses in polar coordinates for this case are given in [1, Eq. (A-4,5), p. 42 and 43]

$$\frac{d\tau}{d\varphi} + \sigma_r - \sigma_\varphi = 0$$

$$\frac{d\sigma_\varphi}{d\varphi} + 2\tau = 0 \qquad (3\text{-}1)$$

$$\frac{d^2}{d\varphi^2}(\sigma_r + \sigma_\varphi) = 0$$

where σ_r , σ_φ are the normal stresses in the r- and φ- directions, while τ is the shear stress. On the surface $\varphi = 0$, the boundary conditions are

$$\sigma_\varphi(0) = -p \qquad \tau(0) = 0 \qquad (3\text{-}2)$$

while behind the compaction front, at $\varphi = \beta$, the conditions (2-35) obtained in Section IIb apply. Noting that the coordinates x, y, z in these conditions are normal, and parallel to the front, respectively, the stress symbols are to be interpreted as follows:

$$\sigma_{xx} \equiv \sigma_\varphi \quad , \quad \sigma_{yy} \equiv \sigma_r \quad , \quad \sigma_{xy} \equiv \tau$$

such that one has two additional conditions:

$$\sigma_r(\beta) = \frac{\nu}{1-\nu}\ \sigma_\varphi(\beta) \qquad (3\text{-}3a)$$

$$\tau(\beta) = 0\ . \qquad (3\text{-}3b)$$

The solution of the differential equations (3-1) satisfying the two conditions (3-2) may be taken directly from Ref. [1] (Eq. A-7),

$$\sigma_r = -p - D(1 + \cos 2\varphi) - C(2\varphi + \sin 2\varphi)$$

$$\sigma_\varphi = -p - D(1 - \cos 2\varphi) - C(2\varphi - \sin 2\varphi) \qquad (3\text{-}4)$$

$$\tau = D \sin 2\varphi + C(1 - \cos 2\varphi)$$

where C and D are constants to be determined from Eqs. (3-3). It can be verified by substitution that the second of these equations is satisfied if

$$C = -N \cos \beta \qquad D = N \sin \beta \tag{3-5}$$

where N is a new constant to be determined from the remaining boundary condition (3-3a). Substitution of Eqs. (3-5) and (3-3a) into Eqs. (3-4), gives two simultaneous linear equations on N and $\sigma_\varphi(\beta)$. Determining $\sigma_\varphi(\beta)$ one finds

$$\sigma_\varphi(\beta) = \frac{-(1-\nu)\,p}{\nu + (1-2\nu)\,\beta \cot \beta} \tag{3-6}$$

This equation contains the still unknown angle β. To determine the latter the relation (2-39) for the velocity U of the shock and compaction front is to be used (note $\sigma_{xx} \equiv \sigma_\varphi$)

$$U^2 = \frac{-\sigma_\varphi(\beta)}{\rho c} \tag{3-7}$$

The velocity U of the front must be the component at a right angle to this front of the velocity V of the load, requiring

$$U = V \sin \beta \tag{3-8}$$

Eqs. (3-6, 7, and 8) give

$$V^2 = \frac{p}{\rho c} \; \frac{1-\nu}{\nu \sin^2 \beta + (1-2\nu) \sin \beta \cos \beta} \tag{3-9}$$

This equation defines β in terms of V. It is simpler, however, to use this equation to compute V for given values of β. If the relationship between V and β is plotted for meaningful values of $0 < \nu < \frac{1}{2}$, a curve of the type shown in Figure 10 for $\nu = 1/3$ is obtained. The velocity V has a minimum, V_{cr}, and

there are two values of the angle β for each value $V > V_{cr}$. The critical minimum value of V occurs for a critical value of the wedge angle $\beta_{cr} < \pi/2$. (There are also values $\beta > 2.03$ in Fig. 10 where $V^2 < 0$. This range of imaginary velocities V is physically meaningless.)

β as function of V is double-valued, but can be made single-valued through elimination of one of the values β by qualitative reasoning. One is interested in a steady state which is the long-time solution to a load p applied to an expanding region, such that β should be less than $\pi/2$, Figure 11. If $\beta > \pi/2$, Figure 12, one would find the following unreasonable situation. Just behind the shock front, the particle velocity is necessarily at right angles to the front, and in case of Figure 12, the velocity would be upward. As the particle velocity further behind the front changes only slightly from the value at the front, the downward loads p would produce upward velocities, which is not possible. Among the steady-state solutions contained in Eq. (3-9), those for $\beta > \pi/2$, while mathematically correct, are physically not appropriate. By reasoning further, that, in the range $\infty > V \geq V_{cr}$ where solutions exist at all, the solutions ought to be continuous, we conclude that the solutions for angles in the range $\beta_{cr} < \beta < \pi/2$ should also be eliminated, and only the range

$$0 < \beta \leq \beta_{cr} \tag{3-10}$$

furnishes meaningful solutions. In the example, Figure 10, the applicable values of V are shown as a solid line. The value of β_{cr} can be found by differentiation of Eq. (3-9), which leads to the condition

$$\frac{\tan(2\beta_{cr})}{\beta_{cr}} = -2(1-2\nu) \tag{3-11}$$

The fact that no steady-state solution was found if the velocity V is less than a critical value, V_{cr} , requires discussion. If one considers the problem of a half-space subjected to an expanding load p, the solution may have the character shown in Figure 11, where the locking front and the leading edge of the pressure p meet at point A. However, it is also possible that the locking front is a "detached" front, Figure 13, moving ahead of the load p. In this case the "steady-state" solution, which is an approximate solution near the front of the applied load, point A, is simply the Huth-Cole solution [6], because in the vicinity of A the material is elastic and the compaction front has moved far away.

Substituting β_{cr} from Eq. (3-11) into Eq. (3-9), it will be noted that V^2 is proportional to $p/\rho\epsilon$ such that the critical velocity V_{cr} is proportional to $\sqrt{p}$, and V_{cr} increases with the applied pressure.

Equation (3-6) permits the determination of the stress σ_φ at the locking front, the value of which may be shown to be the maximum of σ_φ anywhere. Figure 14 gives a plot of $-\sigma_\varphi/p$ as function of V, indicating that σ_φ varies only slightly, from unity for $V = \infty$, up to $\sigma_\varphi = 1.37$ for $V = V_{cr}$.

Case B. After Locking, the Material is Elastic, but Subject to Slip.

For this material, the conditions at the compaction front have been considered in Section IIc. The relations between the stresses at the front depend on the relative values of Poisson's ratio ν and of the material parameter k.

If, see Eq. (2-51),

$$\frac{\nu}{1-\nu} \leq k \tag{3-12}$$

slip will occur in an infinitely thin region immediately at the locking front, and the relations between the normal and tangential stresses immediately behind the front are given by Eq. (2-50). If on the other hand,

$$\frac{\nu}{1-\nu} > k \tag{3-13}$$

the material at the front will remain elastic, and Eq. (2-35) applies.

Consider first materials where Eq. (3-12) holds, such that Eq. (2-50) applies. Using again the system of polar coordinates r, φ shown in Fig. 9, the state of stress in the wedge-shaped region $0 \leq \varphi \leq \beta$ will be subject to the following boundary conditions:

$$\sigma_r(\beta) = k\,\sigma_\varphi(\beta) \tag{3-14a}$$

$$\tau(\beta) = 0 \tag{3-14b}$$

$$\sigma_\varphi(0) = -\,p \tag{3-14c}$$

$$\tau(0) = 0 \tag{3-14d}$$

In the interior of the wedge, the behavior of the material was described in Section IIc by a set of equations and inequalities, Eqs. (2-40 to 44). To simplify the present treatment materials without cohesion will be considered, such that the quantity s in Eq. (2-41) vanishes, s = 0.

Equations (3-14) give conditions for the stresses at the boundaries of the wedge formed by the surface and by the compaction front, but the determination of the stresses within the wedge is complicated by the fact that one does not know in this stage in what portion of the wedge slip occurs, and in what portions the material will act elastically. It will be demonstrated hereafter that elastic behavior occurs everywhere in the interior of the wedge.

To show this, the elastic solution will be obtained from the differential Eqs. (3-1) used in Section A, in conjunction with the boundary conditions (3-14) appropriate for the case of slip at the compaction front.

Noting that the present boundary conditions (3-14c, d) are identical with Eqs. (3-2) in Section A, the solution (3-4) of the differential Eqs. (3-1) applies again,

$$\begin{aligned} \sigma_r &= -p - D(1 + \cos 2\varphi) - C(2\varphi + \sin 2\varphi) \\ \sigma_\varphi &= -p - D(1 - \cos 2\varphi) - C(2\varphi - \sin 2\varphi) \\ \tau &= D \sin 2\varphi + C(1 - \cos 2\varphi) \end{aligned} \tag{3-15}$$

where the arbitrary constants C and D will be determined from the boundary conditions (3-14a, b). The second of these conditions is satisfied if

$$C = -N \cos \beta \qquad D = N \sin \beta \tag{3-16}$$

where N is a new constant to be determined from Eq. (3-14a). Substitution of Eqs. (3-14a) and (3-16) into Eq. (3-15) for $\varphi = \beta$ gives two simultaneous equations on N and $\sigma_\varphi(\beta)$. One finds

$$\sigma_\varphi(\beta) = \frac{-p}{k + (1-k)\,\beta \cot \beta} \tag{3-17}$$

and

$$N = \frac{p}{2\beta \cos \beta + \frac{2k}{1-k} \sin \beta} \tag{3-18}$$

To confirm the claim that the stresses everywhere in the wedge are such that no slip occurs and that the solution (3-15) is appropriate, it is convenient to express the stresses σ_r , σ_φ and τ in terms of the principal stresses

σ_1 and σ_2 and of the angle $\gamma = \gamma(\varphi)$ which the direction of σ_1 makes with the radial, Figure 15. Proceeding similar to the approach in [1, p. 43, Eqs. (A-8 to 10)], the principal stresses σ_1 and σ_2 are expressed by two functions of φ, namely $\sigma = \sigma(\varphi)$ and $\bar{k} = \bar{k}(\varphi)$,

$$\begin{aligned} \sigma_1 &= -\sigma \\ \sigma_2 &= -\bar{k}\sigma \end{aligned} \tag{3-19}$$

Using the conventional expressions for the stresses in terms of the principal stresses, one finds

$$\begin{aligned} \sigma_r &= \sigma_1 \cos^2\gamma + \sigma_2 \sin^2 \gamma = -(1-\bar{k})\sigma \cos^2\gamma - \bar{k}\sigma \\ \sigma_\varphi &= \sigma_1 \sin^2\gamma + \sigma_2 \cos^2 \gamma = -(1-\bar{k})\sigma \sin^2\gamma - \bar{k}\sigma \\ \tau &= (\sigma_1 - \sigma_2) \sin \gamma \cos \gamma = -(1-\bar{k})\sigma \sin \gamma \cos \gamma \end{aligned} \tag{3-20}$$

Elimination of σ and $\bar{k}$ from these equations yields a relation between σ_r, σ_φ, τ and γ

$$\tau - \frac{\sigma_r - \sigma_\varphi}{2} \tan 2\gamma = 0 \tag{3-21}$$

Alternatively, σ may be eliminated from the first two Eqs. (3-20) with the result

$$\frac{1-\bar{k}}{1+\bar{k}} = \frac{1}{\cos 2\gamma} \frac{\sigma_r - \sigma_\varphi}{\sigma_r + \sigma_\varphi} \tag{3-22}$$

The stresses σ_r, σ_φ and τ for any value of φ are given by Eqs. (3-15) if the values of C, D, and N from Eqs. (3-16, 18) are substituted. To show that no slip occurs in the interior of the wedge, it will be shown that the

ratio of the principal stresses obtained from Eqs. (3-19)

$$\sigma_2/\sigma_1 = \bar{k} \tag{3-23}$$

remains within required limits. If σ_1 is the major stress, $-\sigma_1 \geq -\sigma_2$ slip will not occur if $\bar{k} > k$. However, the formulation (3-20) does not assure that σ_1 is the major principal stress. If σ_2 is the major stress, slip will not occur if $\bar{k} < 1/k$, such that the general requirement for elastic behavior without slip becomes

$$1/k > \bar{k} > k \tag{3-24}$$

In similarity to [1, Appendix A], this inequality will be confirmed step by step in various locations. As a first step, the behavior of the function $\bar{k}(\varphi)$ near $\varphi = \beta$ is considered.

Due to the boundary conditions (3-14a, b), σ_φ and σ_r in the location $\varphi = \beta$ are the major and minor principal stresses, respectively, such that by selecting $\sigma_\varphi = \sigma_1$ the values of $\bar{k}(\beta)$ and $\gamma(\beta)$ become:

$$\bar{k}(\beta) = k \tag{3-25a}$$

$$\gamma(\beta) = \pi/2 \tag{3-25b}$$

To determine the sign of the derivative of $\bar{k}$ near $\varphi = \beta$, Eqs. (3-16) are substituted into Eqs. (3-15), and the result is substituted into Eq. (3-22):

$$\frac{1-\bar{k}}{1+\bar{k}} = \frac{N \sin(\beta - 2\varphi)}{\cos 2\gamma[p + N(\sin \beta - 2\varphi \cos \beta)]} \tag{3-26}$$

Taking the derivative of this expression with respect to φ, noting Eq. (3-25b), and that N according to Eq. (3-18) does not depend on φ, one finds

$$\frac{d}{d\varphi}\left(\frac{1-\bar{k}}{1+\bar{k}}\right)_{\varphi=\beta} = \frac{4N^2 \sin\beta \cos\beta}{[p + N(\sin\beta - 2\beta\cos\beta)]^2} \tag{3-27}$$

N being a real number, the sign of the above expression in the range $0 < \beta < \pi$ is necessarily controlled by the term $\cos\beta$, or

$$\text{sign}\ \frac{d}{d\varphi}\left(\frac{1-\bar{k}}{1+\bar{k}}\right)_{\varphi=\beta} = \text{sign}\ [\cos\beta] \tag{3-28}$$

The value of $\bar{k}(\beta) = k$ is by definition in the range $0 < k < 1$, as consequence of which the sign of the derivative of $\bar{k}$ and of $\frac{1-\bar{k}}{1+\bar{k}}$ are opposite, or finally

$$\text{sign}\ [\bar{k}'(\beta)] = \text{sign}\ [-\cos\beta] \tag{3-29}$$

Equation (3-24) requires that the value of $\bar{k}(\varphi)$ in the interior of the wedge must be larger than the value at the boundary, $\bar{k}(\beta) = k$, such that the derivative $\bar{k}'(\beta)$ must be negative. Eq. (3-29) gives therefore $\cos\beta > 0$, restricting the validity of the elastic solution to wedge angles

$$0 < \beta < \pi/2 \tag{3-30}$$

Next, Eq. (3-21) defines $\tan(2\gamma)$ as function of the stresses. Using Eqs. (3-15 and 16) one finds

$$\tan(2\gamma) = \frac{2\sin\varphi\sin(\beta-\varphi)}{\sin(2\varphi - \beta)} \tag{3-31}$$

In the range of β given by Eq. (3-30) the function on the right-hand side vanishes for $\varphi = 0$ and $\varphi = \beta$, assumes negative (positive) values for $0 < \varphi < \beta/2$ ($\beta/2 < \varphi < \beta$), and becomes infinite for $\varphi = \beta/2$. Solving for 2γ gives an infinite set of solutions. Starting with a value $2\gamma(0) = \pm n\pi$, where n is an arbitrary integer, 2γ decreases from above starting value for $\varphi = 0$ to an end value

$2\gamma(\beta) = (\pm\, n\text{-}1)\,\pi$. [It is easily checked that $\tan(2\gamma)$ goes through the same range of values as the right side of Eq. (3-31).] Eq. (3-25b), defines the value $\gamma(\beta) = \pi/2$, such that the appropriate value of n must be n = 2, and

$$\gamma(0) = \pi \tag{3-32}$$

The angle γ defining the direction of the principal stress decreases gradually from $\gamma(0) = \pi$ to $\gamma(\beta) = \pi/2$.

Equation (3-32) defines the position of the principal stress σ_1 for $\varphi = 0$. Referring to Fig. 15, σ_1 acts in the radial direction, or $\sigma_1 = \sigma_r(0)$. The other principal stress is then $\sigma_2 = \sigma_\varphi(0)$. These relations, together with Eqs. (3-15, 16 and 18) permit determination of the value $\bar{k}(0)$ from Eq. (3-23):

$$\bar{k}(0) = \frac{\sigma_2}{\sigma_1} = \frac{\sigma_\varphi(0)}{\sigma_r(0)} = \frac{p}{p + 2N \sin\beta} = \frac{(1\text{-}k) + 2k\,\dfrac{\tan\beta}{\beta}}{(1\text{-}k) + (1\text{+}k)\,\dfrac{\tan\beta}{\beta}} \tag{3-33}$$

The angle β being limited by Eq. (3-30) to $0 < \beta < \pi/2$ and the material property k being limited, $0 < k < 1$, numerator and denominator are each the sum of two positive terms. Further, in the permissible range of β the value of $\tan\beta/\beta > 0$, and since $2k < 1+k$, the value of the fraction in Eq. (3-33) cannot possibly exceed unity, $\bar{k}(0) \leq 1$. The smallest value of the fraction occurs when $\tan\beta/\beta$ is as large as possible, i.e., $\tan\beta/\beta \to \infty$, which case gives a lower limit, $\bar{k}(0) \geq 2k/(1+k)$. In turn, $1+k < 2$, such that $2k/(1+k) > k$, or finally

$$1 \geq \bar{k}(0) > k \tag{3-34}$$

The condition for elastic behavior, Eq. (3-24), is therefore satisfied at $\varphi = 0$.

As next step the sign of the derivative $\bar{k}'(0)$ is determined by differentiation of Eq. (3-26). Noting Eq. (3-32), one finds

$$\frac{d}{d\varphi}\left(\frac{1-\bar{k}}{1+\bar{k}}\right)\Bigg|_{\varphi=0} = -\frac{2p\ N\cos\beta}{[p + N\sin\beta]^2} \tag{3-35}$$

In the range (3-30), the values of $\cos\beta$ and of N, the latter defined by Eq. (3-18), are positive, such that the above derivative is negative. The sign of the derivative $\bar{k}$ being opposite to that of $\frac{1-\bar{k}}{1+\bar{k}}$,

$$\text{sign}\ [\bar{k}'(0)] > 0 \tag{3-36}$$

The results obtained so far may be summarized by considering Fig. 16 which shows a typical plot of $\bar{k}(\varphi)$. The end points of the curve have been determined above, $\bar{k}(0)$ being limited by the inequality (3-34), while $\bar{k}(\beta) = k$. Equations (3-29, 30 and 36) define the tangents to the curve $\bar{k}(\varphi)$ at $\varphi = 0$ and $\varphi = \beta$ in the manner shown in Fig. 16. Between these end points $\bar{k}(\varphi)$ is defined by Eq. (3-26) as a function of φ. The form of this equation is, however, not suitable to demonstrate that $k(\varphi)$ is a smooth function, as indicated in Fig. 16. If Eq. (3-26) is used, the function $\sin(\beta - 2\varphi)/\cos 2\gamma$ becomes indefinite for $\varphi = \beta/2$ when $\gamma(\beta/2) = 3\pi/4$. This difficulty is overcome by computing the value of $\sin(\beta - 2\varphi)$ from Eq. (3-31) and substituting the result into Eq. (3-26),

$$\frac{1-\bar{k}}{1+\bar{k}} = \frac{-2N\sin\varphi\sin(\beta-\varphi)}{\sin 2\gamma}\ \frac{1}{p + N(\sin\beta - 2\varphi\cos\beta)} \tag{3-37}$$

The first fraction on the right side of this equation is obviously smooth, because γ varies smoothly from $\gamma(0) = \pi$ to $\gamma(\beta) = \pi/2$, see Eq. (3-32) and the adjoining text. Excluding the end values $\gamma(0)$ and $\gamma(\beta)$, the value of $\sin 2\gamma < 0$, and because $N > 0$, as previously noted in connection with Eq. (3-35), the first fraction is necessarily positive.

To recognize the character of the second fraction, the value of N, Eq. (3-18), is substituted

$$\frac{1}{p + N(\sin\beta - 2\varphi\cos\beta)} = \frac{2\beta\cos\beta + \frac{2k}{1-k}\sin\beta}{p[2(\beta-\varphi)\cos\beta + \frac{1+k}{1-k}\sin\beta]} \tag{3-38}$$

In the range $0 < \beta < \pi/2$ all terms on the right side are positive, and the fraction (3-38) is necessarily positive. Returning to Eq. (3-37) it follows that

$$\frac{1-\bar{k}}{1+\bar{k}} > 0 \tag{3-39}$$

If the maximum value of $\bar{k}$, indicated in Fig. 16, were larger than unity, the expression $\frac{1-\bar{k}}{1+\bar{k}}$ would become negative, such that Eq. (3-39) indicates that

$$\max \bar{k}(\varphi) < 1 \tag{3-40}$$

Allowing for the minimum of $\bar{k}(\varphi)$ at $\varphi = \beta$, $\min \bar{k} = k$, the values $\bar{k}(\varphi)$ satisfy Eq. (3-24). It has therefore been proved that the original assumption that slip does not occur in the wedges, $0 \leq \varphi < \beta$, is justified and furnishes the solution to the problem considered.

To complete the analysis, we obtain the inclination β of the locking front as function of the velocity V of the surface pressure from Eqs. (3-7 and 8) used in the elastic case. One finds

$$V^2 = \frac{\frac{p}{\rho c}}{k\sin^2\beta + (1-k)\beta\sin\beta\cos\beta} \tag{3-41}$$

Just as in the elastic case, Eq. (3-9), V as function of β may be plotted, and the result, shown for $k = 1/3$ in Fig. 17, is quite similar to the one for the elastic case, except that Eq. (3-30) restricts the values of the angle β to the range $0 < \beta < \pi/2$. Real values of V are found everywhere in this range. These values of V have a minimum V_{cr}, which occurs for a critical wedge angle, $\beta_{cr} < \pi/2$. The latter may be found from

$$\frac{\tan(2\beta_{cr})}{\beta_{cr}} = -\frac{2(1-k)}{1+k} \tag{3-42}$$

Figure 17 shows that for values of V near V_{cr} there are two values of β, one larger, one smaller than β_{cr}. However, using the reasoning employed in the elastic case [in the text following Eq. (3-9)], it is concluded that only wedge angles $\beta \leq \beta_{cr}$ are physically meaningful. The inapplicable portion of the curve in Fig. 17 is shown in dashed lines.

The fact that no solution has been obtained if $V < V_{cr}$ is again ascribed to the fact that a steady state solution for an expanding surface load need not have the character of Fig. 11, where the locking front and the face of the applied pressure move together. For velocities below the critical, a detached locking front forms, Fig. 13, and the steady state solution is given by [6]. In applications the velocity V of shock waves in air is always larger than V_{cr}, such that detached locking fronts are merely an academic possibility. The solutions derived above apply therefore in cases of practical interest, as may be seen from the typical example at the end of Section IV.

It is necessary to remember that the solution just obtained, shown in Fig. 17 for $k = 1/3$, applies only if the inequality (3-12) is satisfied. For the example, $k = 1/3$, this requires $\nu \leq 1/4$. The alternative case, when the inequa-

lity (3-13) applies remains to be discussed. If the latter inequality,

$$\frac{\nu}{1-\nu} > k$$

applies, the stresses at and immediately behind the consolidation front are elastic, such that the conditions at the boundaries of the wedge are exactly those used for the elastic half-space, Eqs. (3-2) and (3-3). It will be shown that the elastic solution found in Section A for these boundary conditions, represents a state of stress in which condition (2-43) is satisfied everywhere, i.e. no slip occurs in any location. This means, that the solution for an elastic material not subject to slip applies in case of the inequality (3-13) also for the material subject to slip.

To prove above contention, it is noted that the solution in Section A (for the elastic material) may be obtained from the solution for the material subject to slip by replacing the value k by the expression $\nu/(1-\nu)$. This is due to the fact that the only difference in the formulation of the two solutions originates from the boundary conditions for $\sigma_r(\beta)$, Eq. (3-3a) and Eq. (3-14a), respectively, where in one case the term $\nu/(1-\nu)$ occurs, while k occurs in the other. The results concerning the value of the function $\bar{k}(\varphi)$ obtained above, Eqs. (3-19) to (3-42), can therefore be utilized without further computations. Figure 18 shows a typical distribution of $\bar{k}(\varphi)$. At the boundary $\varphi = \beta$, the ratio $\bar{k}(\beta)$ of the two principal stresses is, by virtue of Eq. (3-3a),

$$\bar{k}(\beta) = \frac{\nu}{1-\nu} > k \tag{3-43}$$

The end point of the $\bar{k}$-curve at β is therefore above k. Further, the value $\bar{k}(\beta)$ must be less than unity, because Poisson's ratio is always less than 1/2.

Replacing k by $\nu/(1-\nu)$ does not affect the results obtained in Eq. (3-29), Eq. (3-34), Eq. (3-36) and Eq. (3-40), defining, respectively, $\bar{k}'(\beta)$, $\bar{k}(0)$, $\bar{k}'(0)$ and max $\bar{k}$. The values $\bar{k}(\varphi)$ lie therefore everywhere between the limits

$$k < \bar{k}(\varphi) < 1 \tag{3-44}$$

confirming the claim made above that slip does not occur anywhere.

While this was previously stated, it is stressed again that all results in this Section, for Case A as well as Case B, apply only for velocities V below a certain limit. This is due to the fact that, in similarity to [1], the equations of motions in the elastic, wedge-shaped regions were approximated by Eqs. (3-1). This approximation is reasonable only if the velocity V is a fraction of the velocity of P-waves

$$c_p^2 = \frac{E(1-\nu)}{\rho(1+\nu)(1-2\nu)} \tag{3-45}$$

where E and ν are the elastic constants describing the behavior of the material after compaction, if no slip occurs. It was shown in [1] that the approximate Eqs. (3-1) may be used if $V/c_p < 0.20$, such that the present results will apply in this range. However, for values of the parameters of interest in applications, the locking front makes a very small angle with the surface, $\beta < 0.20$ (see the example at the end of Section IV). A comparison with a refined solution shows that for such small angles of β, and for reasonable values of Poisson's ratio, $\nu \leq 1/3$, the use of Eqs. (3-1) is permissible even for values of V/c_p higher than 0.20. The present solution is expected to give good results if the inequalities

$$\nu \leq 1/3 \quad , \quad \beta \leq 0.20 \tag{3-46}$$

and

$$V/c_p < 0.50 \tag{3-47}$$

are satisfied. These inequalities insure that $V > c_s$, where $c_s = \sqrt{G/\rho}$ is the velocity of shear waves in the elastic (compacted) material. c_s being about 0.60 to 0.70 c_p , the present solution applies for a major portion of the "subseismic" range, $V < c_s$.

IV DISCUSSION OF RESULTS

In the previous Section, Case B, the stresses in a half-space were obtained for locking materials of elastic-Coulomb slip behavior after compaction. It was found that two situations must be distinguished, and the results differ, depending on whether

$$\frac{\nu}{1-\nu} \leq k \tag{4-1}$$

or

$$\frac{\nu}{1-\nu} > k \tag{4-2}$$

The solutions obtained indicate that a locking front occurs, inclined at an angle β, Fig. 19, when the velocity V of the applied surface load p exceeds a critical value V_{cr} . The value $\sigma_\varphi(\beta)$ of the normal stress at the front, the relations between V and β, and the value of β_{cr} are given, respectively, by Eqs. (3-17, 41, 42) in the case of the inequality (4-1), and Eqs. (3-6, 9, 11) in the case of (4-2). It was further concluded that only values of $\beta \leq \beta_{cr}$ are physically meaningful. Figure 17 shows a typical plot of $V(\beta)$ for $k = 1/3$ when Eq. (4-1) applies, while Figs. 10 and 14 present $V(\beta)$ and $\sigma_\varphi(\beta)$, respectively, for $\nu = 1/3$ in case Eq. (4-2) holds.

The details of the solution show that, regardless whether Eq. (4-1) or (4-2) applies, no slip occurs in the interior of the wedge-shaped areas $0 \leq \varphi < \beta$, which act entirely elastic. However, in the case of Eq. (4-1) slip does occur within the (theoretically infinitely thin) compaction front. In the case of Eq. (4-2) slip does not occur at all, not even at this front.

From the results concerning the stress field, other quantities of interest can be obtained. One important quantity is the permanent strain produced at any point due to the passing of the pressure front on the surface. The significant portion of the permanent strain occurs during the passing of the locking front, the principal strains being

$$\epsilon_1 = -\epsilon \quad , \quad \epsilon_2 = 0 \tag{4-3}$$

where ϵ is the locking strain, while ϵ_1 , ϵ_2 are inclined at angles to the surface of $90^\circ - \beta$, and β, respectively. Changes of strain subsequent to the passing of the locking front are negligible compared to the locking strain ϵ, because in an ideal locking material, when no slip occurs, the post-locking elastic strains are of the order $|p/E| << \epsilon$. Equations (4-3) define therefore the total permanent strain. Without interaction of structure and free field an originally circular structure, Fig. 19, would be deformed to an ellipse of the axis ratio $1 - \epsilon$, and the original volume of the structure would be reduced by a factor $1 - \epsilon$. A cylindrical shell, e.g., will not strongly resist the deformation into an ellipse, but may be able to resist a volume change materially. Predictions on the behavior of structures in locking materials require therefore further analysis of interaction effects which will modify the free field results on stress and strain obtained above.

One may also obtain the accelerations a and particle velocities u which correspond to the stress field obtained in Section III. Again, because we consider an ideal locking material, the significant effect is the change in particle velocity at the locking front. Ahead of the front, $u = 0$. To obtain the particle velocity u_L behind the locking front, it is noted that the front is plane, such that the well known relation applying for one dimensional wave propagation

$$u_L = \epsilon U \tag{4-4}$$

may be used, where U is the velocity of the front, and u_L is the particle velocity at right angles to the front after locking. The velocity U is given by Eq. (2-39), where σ_{xx} means the normal stress at the front, in the present situation $\sigma_{xx} \equiv \sigma_\varphi(\beta)$. The particle velocity u_L is therefore

$$u_L = \sqrt{\frac{-\epsilon\sigma_\varphi(\beta)}{\rho}} \tag{4-5}$$

where $\sigma_\varphi(\beta)$ is given by the appropriate Eqs. (3-6) or (3-17). Fig. 20 gives the time history of the particle velocity u(t), its direction making the angle $90^\circ - \beta$ with the surface. The jump occurs when the locking front passes the point of observation. The acceleration a vanishes except at the instance of passing of the front, where $a = \infty$, but the order of the infinity is such that

$$\int a\, dt = u_L \tag{4-6}$$

The direction of a is the same as that of u(t). This result may be used for the determination of shock factors.

For materials which behave elastically after locking, no separate discussion is necessary. Statements and results apply, as given for materials with slip when the inequality (4-2) holds.

Typical Example

Consider a soil of density $\rho = 1.8 \times 10^{-4}$ lb.sec.^{2}/in.^{4} at a pressure level $p = 200$ lb./in.^{2}, when $V = 3970$ ft./sec. Assume a material with slip, $k = 1/3$, $\nu = 1/5$, $\epsilon = 0.02$. The inequality (4-1) holds, such that Eqs. (3-17, 41, 42) apply.

To ascertain that $V_{cr} < V$, one finds from Eq. (3-42): $\beta_{cr} = 1.145$ rad., and from Eq. (3-41) the corresponding value $V_{cr} = 820$ ft./sec. $< V$. Eq. (3-41) will therefore have a root $\beta < \beta_{cr}$ for the above parameters and the analysis presented above furnishes the stresses, velocities, etc., in this situation.

Solving Eq. (3-41) gives $\beta = 0.070$ rad., and Eq. (3-17) furnishes the pressure at the shock front, $\sigma_\varphi(\beta) = 201$ lb./in.^{2} This pressure differs only very slightly from the surface pressure p. This is due to the fact that β is quite small whenever V is very much larger than V_{cr}. The particle velocity behind the locking front, found from Eq. (4-5), is $u_L = 20$ ft./sec.

Due to the fact that the angle β is small, $\beta << 1$, the solution differs only little from the one dimensional one. In the latter the stress at the locking front for an applied step pressure $p = 200$ lb./in.^{2} would also be 200 lb./in.^{2}, while the two dimensional solution gives $\sigma_\varphi(\beta) = 201$ lb./in.^{2}

The analysis presented in Section III is restricted to values of the parameters which satisfy the inequalities (3-46, 47). Eqs. (3-46) are obviously satisfied. Introducing Eq. (3-45) into (3-47) leads to the requirement

$$E > \frac{4\rho(1+\nu)(1-2\nu)}{1-\nu} V^2 \tag{4-7}$$

which gives in the present case $E > 1.5 \times 10^6$ lb./in.^{2} The value E in this inequality is Young's modulus in the compacted material. At the present time there is little factual information on this value of E, for loading or unloading, subsequent to compaction.

In the example discussed above, the velocity V_{cr} was substantially smaller than the shock velocity V in the air. This situation holds generally for a wide range of ϵ and p. This is demonstrated by the following table:

Table of V_{cr} as function of p and ϵ for $k = 1/3$. $\nu \leq 1/4$

ϵ	$p = 100$ lb./in.^{2}	$p = 500$ lb./in.^{2}
0.01	820 ft./sec.	1840 ft./sec.
0.10	260 ft./sec.	580 ft./sec.

The values of V_{cr} are much smaller than the shock velocities in air, $V \sim 2920$ and 6130 ft./sec. for $p = 100$ and 500 lb./in.^{2}, respectively.

V SUMMARY OF CONCLUSIONS

As an introductory step, Section II contains a study of the conditions on locking fronts in problems of two and three dimensional wave propagation. Considering a locking material as a limiting case of a nonlinear (hardening) elastic material, it was found that the normal stress at a locking front must be a principal stress, such that shear stresses vanish.

Based on the study of the conditions on locking fronts, the paper contains an analysis, giving stresses, strains and particle velocities due to a progressing step wave on the surface of a half-space of a locking material, which after compaction is elastic but subject to slip. The slip conditions, previously derived in [1], define the states of stress necessary to overcome internal Coulomb friction in terms of a parameter k, which is the ratio of the minor (compressive) principal stress divided by the major one.

The details of the results, given in Section IV, depend on the relative values of k, and of Poisson's ratio ν as expressed by the inequalities (4-1) and (4-2). There is a locking front, inclined at an angle β, Fig. 19, followed by a gradually varying stress field. Slip occurs only at the locking front if Eq. (4-1) applies, and not at all if Eq. (4-2) applies.

Because of a simplification in the analysis, the results are restricted with respect to the velocity V of the surface pressure. In the case of airblast on the surface of a granular soil, the "Mach number" must be limited to $V/c_p < 0.50$, where c_p is the velocity of P-waves in the compacted material. The velocity c_s of shear waves being only slightly larger than $0.5\ c_p$, the

range of validity of the present solution covers most of the subseismic range, $V < c_s$. Solutions for higher values of V, particularly for the superseismic range, $V > c_p$, require a different approach, left for a future investigation.

As a byproduct of the analysis, the solution for a locking material which, after compaction, acts elastically, without slip, has also been obtained, subject to the limitation $V/c_p < 0.50$.

The example at the end of Section IV indicates that, for airblast, the results of the two dimensional analysis differ only minutely from the results of the much simpler one dimensional analysis. One can expect that this conclusion will also apply for a decaying surface pressure, and one dimensional results may therefore be used approximately for two dimensional problems.

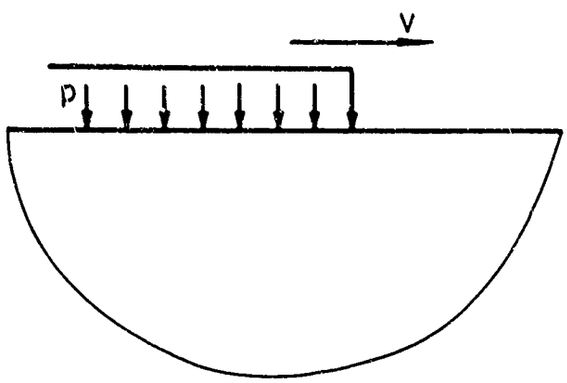

FIG. 1

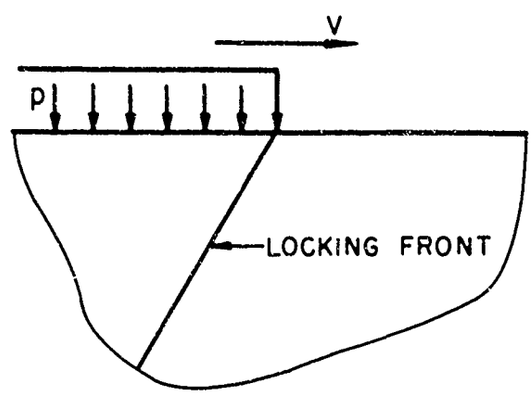

FIG. 2

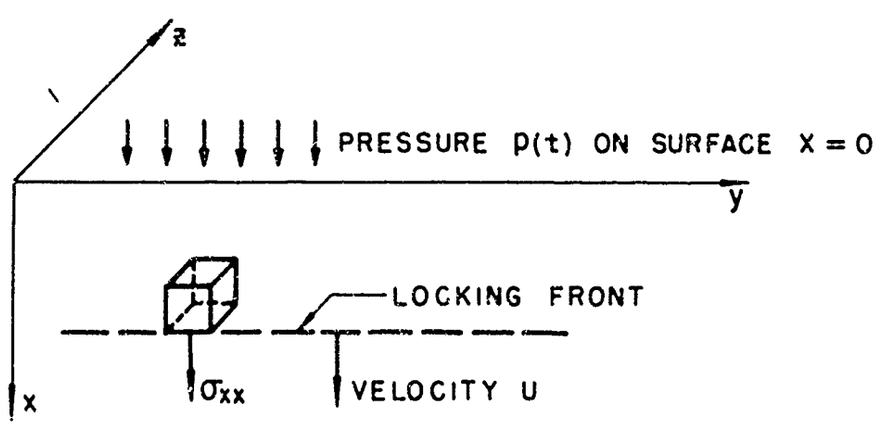

FIG. 3

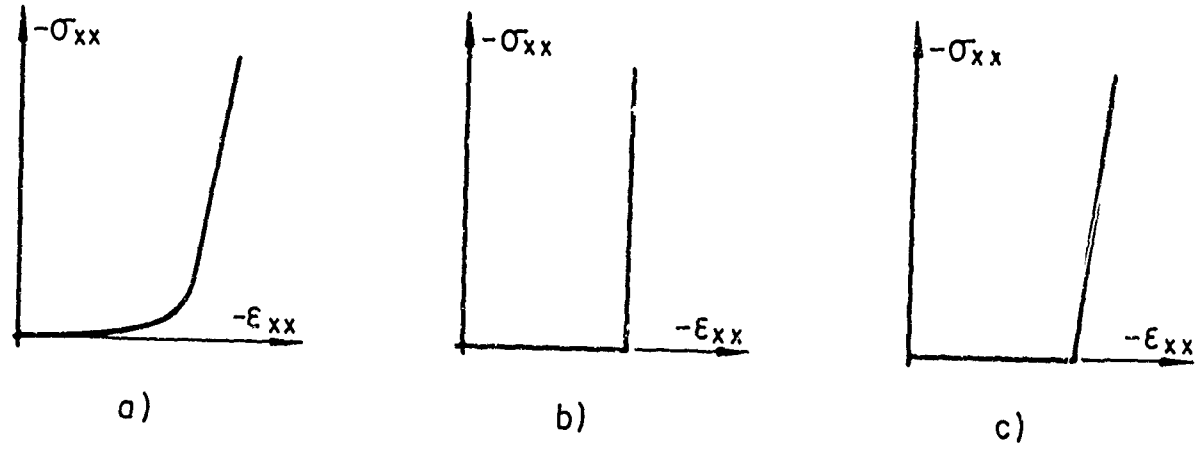
$-\sigma_{xx}$
$-\varepsilon_{xx}$
a)
$-\sigma_{xx}$
$-\varepsilon_{xx}$
b)
$-\sigma_{xx}$
$-\varepsilon_{xx}$
c)

FIG. 4

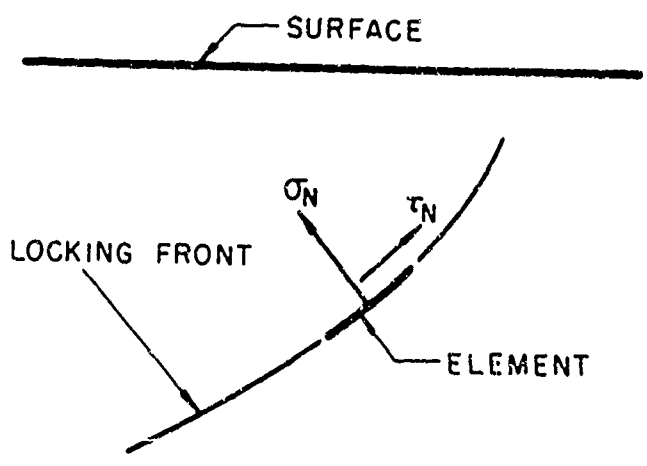
SURFACE
σ_N
τ_N
LOCKING FRONT
ELEMENT

FIG. 5

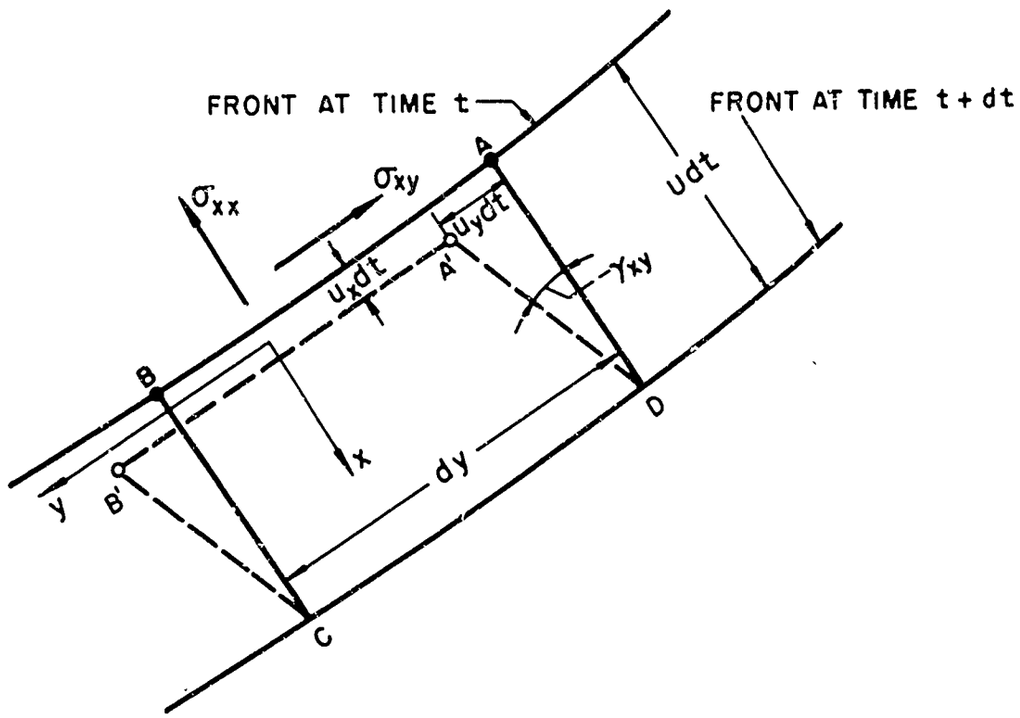
FRONT AT TIME t
FRONT AT TIME t + dt
A
B
C
D
A'
B'
σ_{xx}
σ_{xy}
$u_x dt$
$u_y dt$
γ_{xy}
$u dt$
x
y
dy

FIG. 6

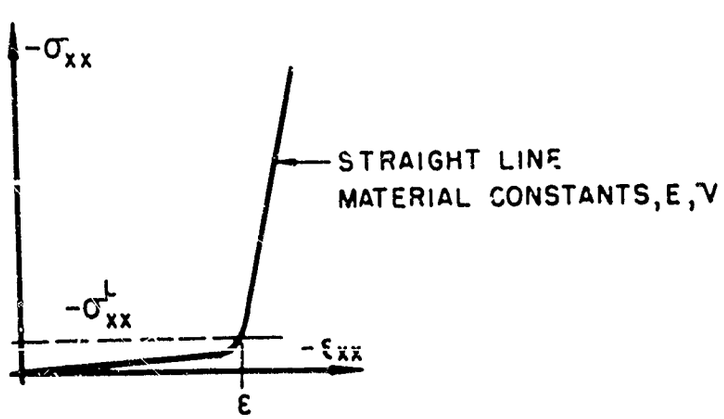
$-\sigma_{xx}$
STRAIGHT LINE
MATERIAL CONSTANTS, E, ν
$-\sigma_{xx}^{L}$
$-\varepsilon_{xx}$
ε

FIG. 7

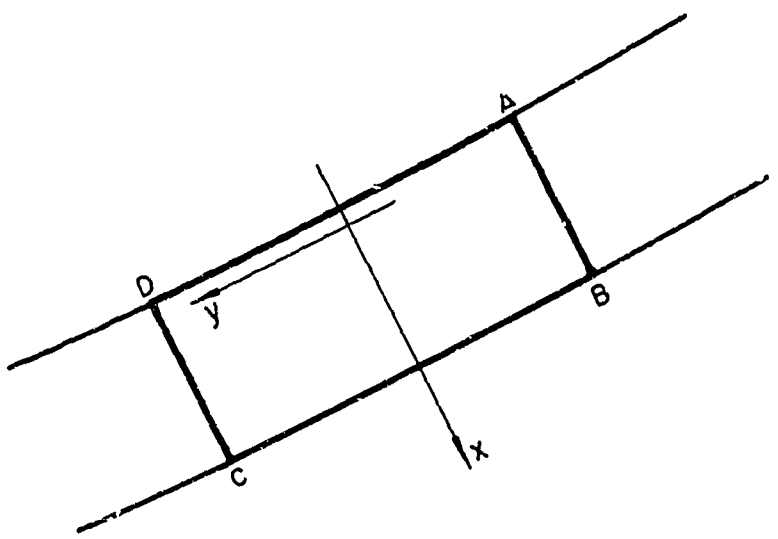

FIG. 8

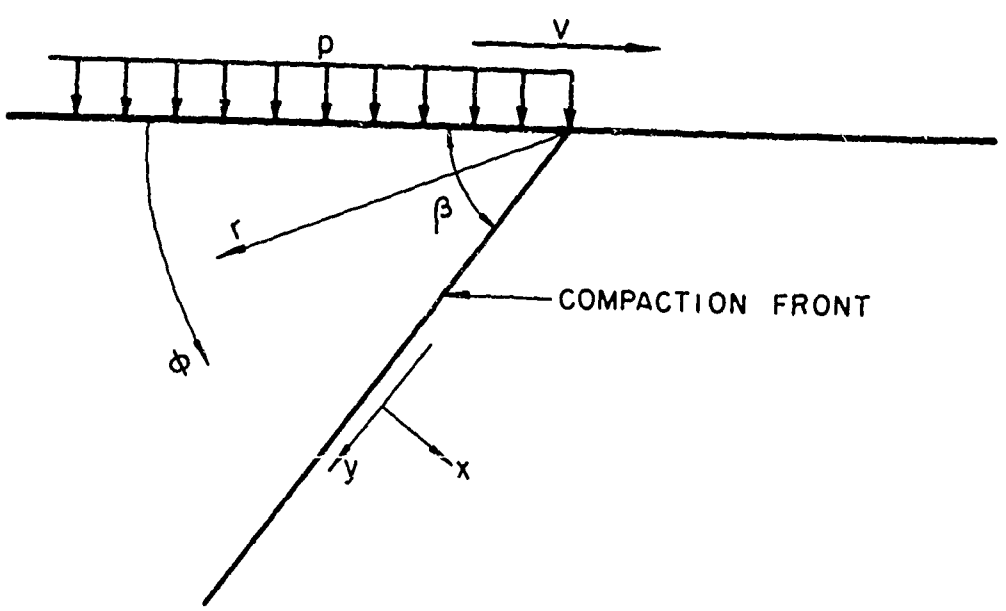

FIG 9

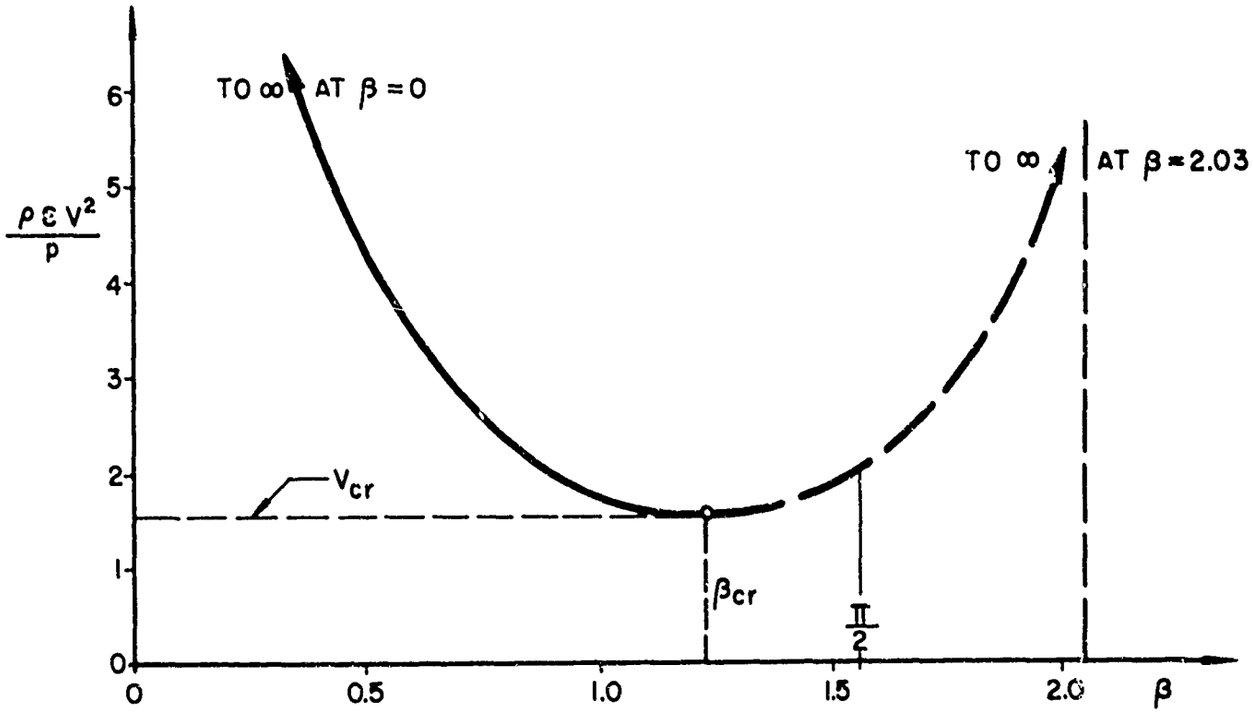

FIG. 10 — V AS FUNCTION OF β (FOR ν=1/3)

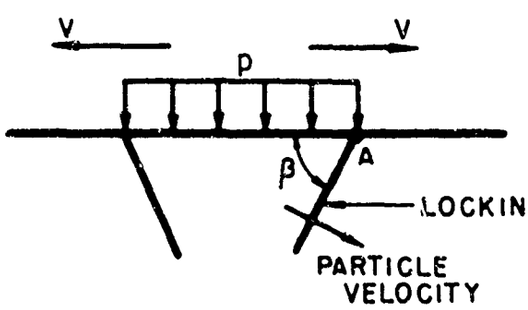

FIG. 11

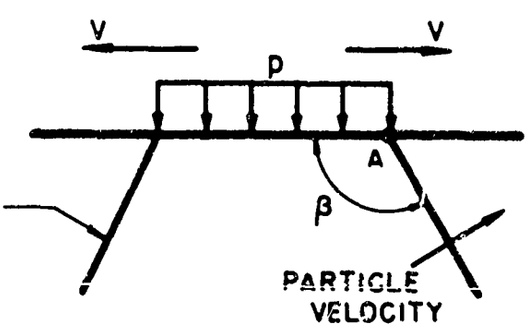

FIG. 12

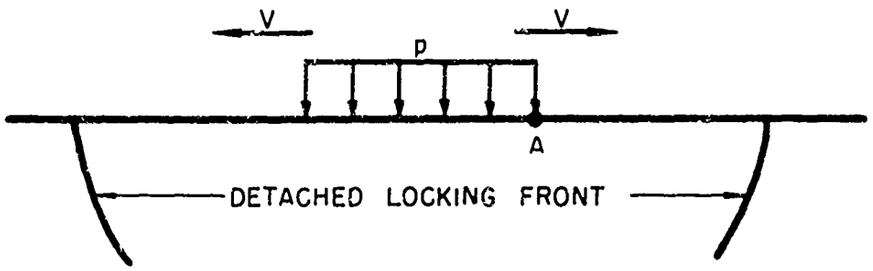

FIG. 13

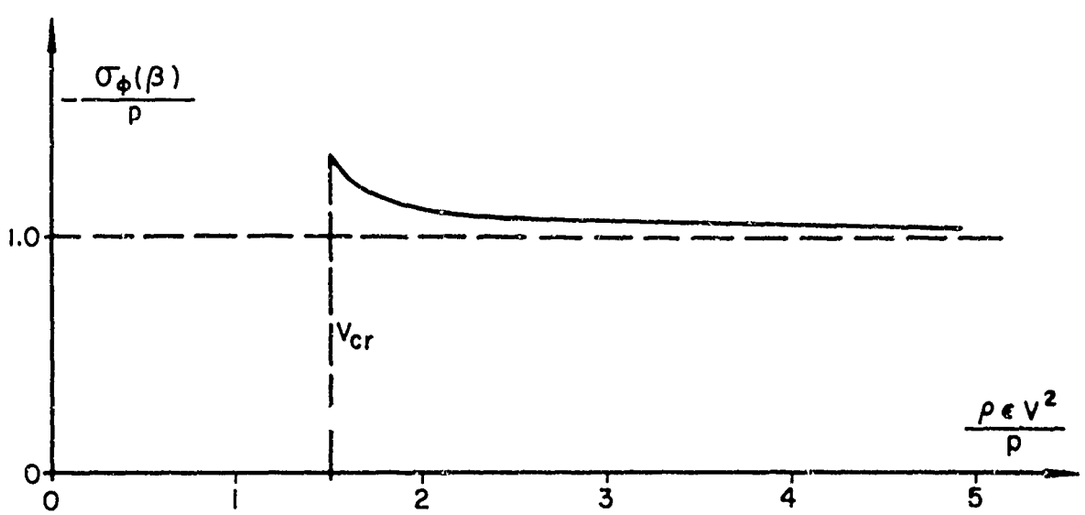

FIG. 14 $\sigma_\phi(\beta)$ AS FUNCTION OF V (FOR $\nu = 1/3$)

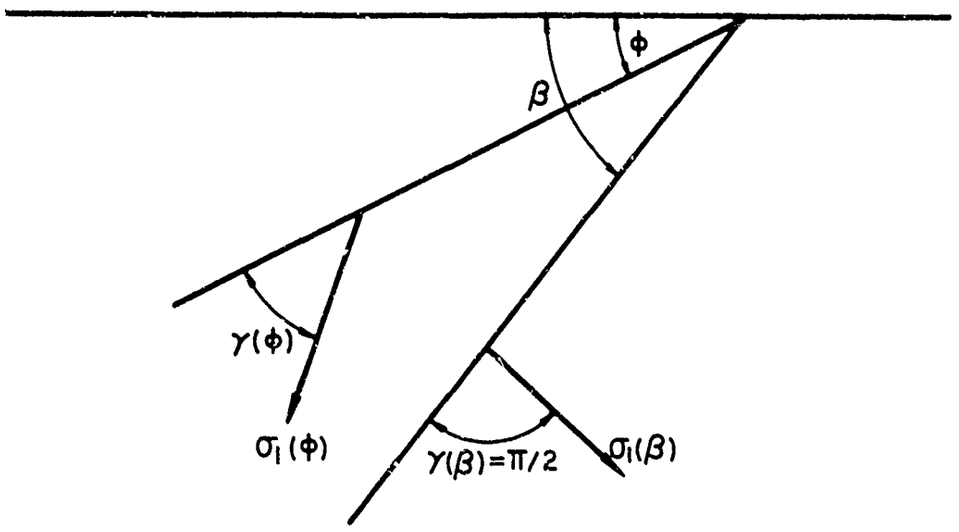

FIG. 15

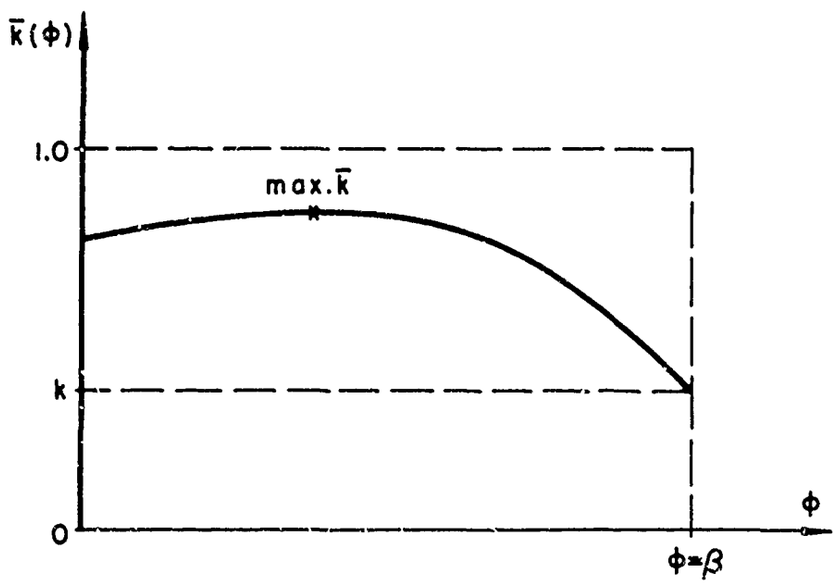

FIG. 16 $\bar{k}(\phi)$ WHEN $\frac{\nu}{1-\nu} \leq k$

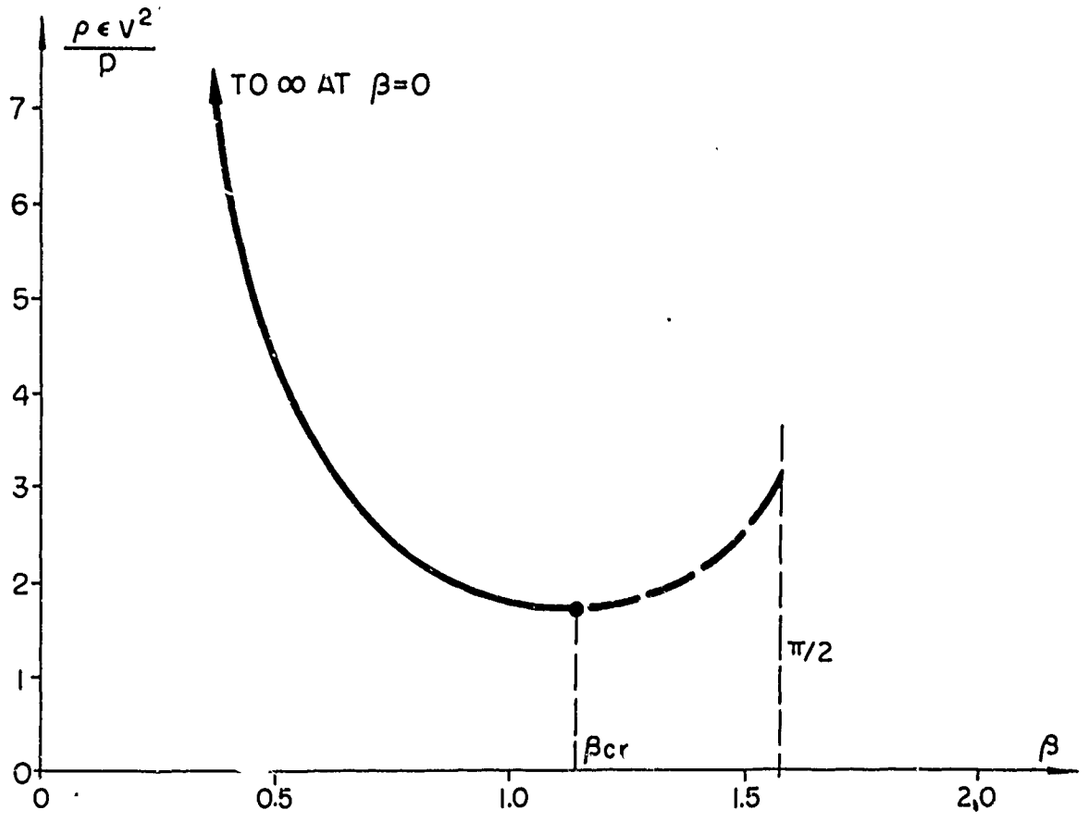

FIG. 17 V AS FUNCTION OF β ($k=1/3$, $\nu \leq 1/4$)

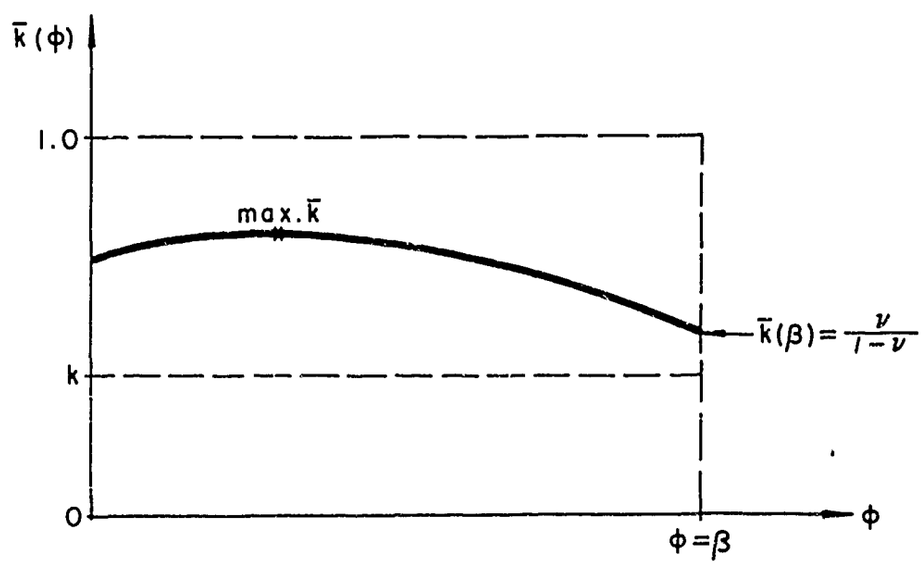

FIG. 18 $\bar{k}(\phi)$ WHEN $\frac{\nu}{1-\nu} > k$

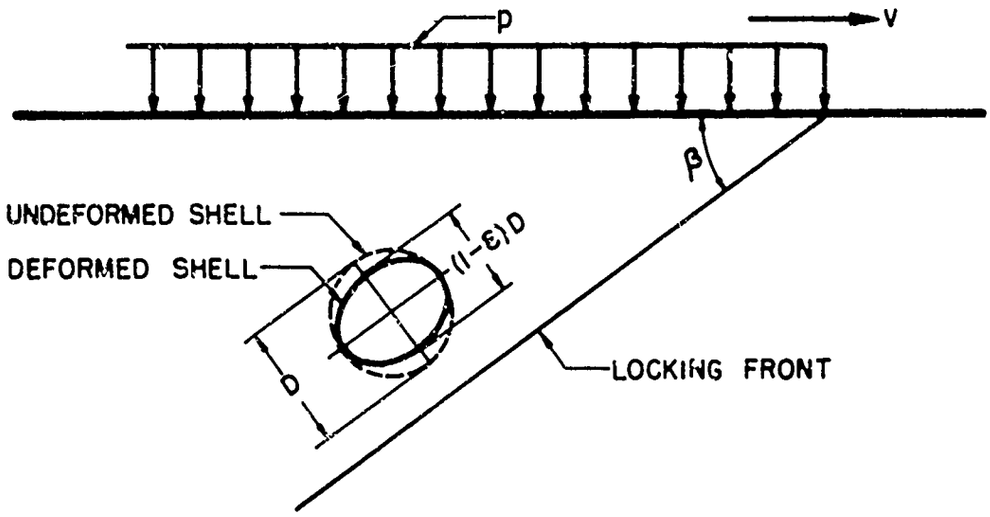

FIG. 19

FIG. 20 PARTICLE VELOCITY u(t)

REFERENCES

[1] H.H. Bleich and E. Heer, Step Load Moving with Low Subseismic Velocity on the Surface of a Half-Space of Granular Material, AFSWC-TDR-63-2, April 1963. (Also, Proceedings ASCE, Vol. 89, No. EM3, June 1963, pp. 97-129.)

[2] M. Salvadori, R. Skalak and P. Weidlinger, Waves and Shocks in Locking and Dissipative Media, Proceedings ASCE, Vol. 86, No. EM2, April 1960.

[3] H.H. Bleich and P. Weidlinger, Final Report on Stress Waves in Granular Materials, AFSWC-RTD-TDR-63-3048, July 1963.

[4] A.E.H. Love, Mathematical Theory of Elasticity, 4th Ed., Cambridge 1927.

[5] A.M. Freudenthal, The Inelastic Behavior of Engineering Materials and Structures, J. Wiley & Sons, New York, 1950.

[6] J. Cole and J. Huth, Stresses Produced in a Half-Plane by Moving Loads, Journal Applied Mechanics, Vol. 25, No. 4, December 1958, p. 433.

DISTRIBUTION

No. cys	
	HEADQUARTERS USAF
	Hq USAF, Wash, DC 20330
2	(AFOCE)
1	(AFRNE-B, Maj Lowry)
1	(AFTAC)
1	USAF Dep, The Inspector General (AFIDI), Norton AFB, Calif 92409
1	USAF Directorate of Nuclear Safety (AFINS), Kirtland AFB, NM 87117
	MAJOR AIR COMMANDS
1	AFSC (SCT), Andrews AFB, Wash, DC 20331
1	AUL, Maxwell AFB, Ala 36112
2	USAFIT, Wright-Patterson AFB, Ohio 45433
1	USAFA, Colo 80840
	AFSC ORGANIZATIONS
1	AFSC Scientific and Technical Liaison Office, Research and Technology Division, AFUPO, Los Angeles, Calif 90045
1	AF Materials Laboratory, Wright-Patterson AFB, Ohio 45433
1	ASD (SEPIR), Wright-Patterson AFB, Ohio 45433
	RTD, Bolling AFB, Wash, DC 20332
1	(RTN-W, Lt Col Munyon)
1	(RTS)
1	AF Msl Dev Cen (RRRT), Holloman AFB, NM 88330
1	AFMTC (MU-135, Tech Library), Patrick AFB, Fla 32925
2	AEDC (AEYD), Arlong AFS, Tenn 37289
	BSD, Norton AFB, Calif 92409
1	(BST)
1	(BSQ)
1	(BSSF)
2	SSD (SSSD), Los Angeles AFS, AFUPO, Los Angeles, Calif 90045
2	ESD (ESTI), L. G. Hanscom Fld, Bedford, Mass 01731
2	APGC (PGOZF), Eglin AFB, Fla 32542
	KIRTLAND AFB ORGANIZATIONS
	AFSWC, Kirtland AFB, NM 87117
1	(SWEH)
5	(SWT)

DISTRIBUTION (cont'd)

No. cys	
	AFWL, Kirtland AFB, NM 87117
15	(WLIL)
5	(WLDC, Lt Higgins)
	OTHER AIR FORCE AGENCIES
2	Director, USAF Project RAND, via: Air Force Liaison Office, The RAND Corporation, 1700 Main Street, Santa Monica, Calif 90406
1	Hq OAR (RROS), Bldg T-D, Wash, DC 20333
1	AFOSR (SRGL), Bldg T-D, Wash, DC 20333
1	AFCRL, L. G. Hanscom Fld, Bedford, Mass 01731
	ARMY ACTIVITIES
1	Director, Ballistic Research Laboratories (Library), Aberdeen Proving Ground, Md 21005
1	Chief of Engineers (ENGMC-EM), Department of the Army, Wash, DC 20315
2	Director, Army Research Office, 3045 Columbia Pike, Arlington, Va 22204
3	Director, US Army Waterways Experiment Sta (WESRL), P. O. Box 631, Vicksburg, Miss 39181
2	Director, US Army Engineer Research and Development Laboratories, ATTN: STINFO Branch, Ft Belvoir, Va
1	US Army Engineer Division, Ohio River, Corps of Engineers, Ohio River Division Laboratories (ORDLBVR), 5851 Mariemont Avenue, Mariemont, Cincinnati 27, Ohio
	NAVY ACTIVITIES
1	Bureau of Yards and Docks, Department of the Navy, Code 22.102, (Branch Manager, Code 42.330), Wash 25, DC
1	Bureau of Ships, Department of the Navy (melvin L. Ball, Code 1500), Wash, DC 20360
1	Commanding Officer and Director, David Taylor Model Basin, Wash 7, DC
1	Superintendent, US Naval Postgraduate School, ATTN: George R. Luckett, Monterey, Calif
2	Commanding Officer and Director, Naval Civil Engineering Laboratory, Port Hueneme, Calif
1	Commander, Naval Ordnance Test Station (Code 753), China Lake, Calif 93557
1	Commander, Naval Ordnance Laboratory, ATTN: Dr. Rudlin, White Oak, Silver Spring, Md 20910
1	Officer-in-Charge, Naval Civil Engineering Corps Officers School, US Naval Construction Battalion Center, Port Hueneme, Calif

DISTRIBUTION (cont'd)

No. cys	
1	Office of Naval Research, Wash, DC 20360
1	Commanding Officer, US Naval Weapons Evaluation Facility (NWEF, Code 404), Kirtland AFB, NM 87117
	OTHER DOD ACTIVITIES
2	Director, Defense Atomic Support Agency (Document Library Branch), Wash, DC 20301
2	Commander, Field Command, Defense Atomic Support Agency (FCAG3, Special Weapons Publication Distribution), Sandia Base, NM 87115
1	Director, Advanced Research Projects Agency, Department of Defense, The Pentagon, Wash, DC 20301
1	Office of Director of Defense Research and Engineering, ATTN: John E. Jackson, Office of Atomic Programs. Rm 3E1071, The Pentagon, Wash, DC 20330
20	DDC (TIAAS), Cameron Station, Alexandria, Va 22314
	AEC ACTIVITIES
1	Sandia Corporation (Information Distribution Division), Box 5800, Sandia Base, NM 87115
1	Sandia Corporation (Technical Library), P. O. Box 969, Livermore, Calif 94551
	OTHER
1	OTS (CFSTI, Chief, Input Section), Sills Bldg, 5285 Port Royal Road, Springfield, Va 22151
1	Office of Assistant Secretary of Defense (Civil Defense), Wash, DC 20301
1	Massachusetts Institute of Technology, Lincoln Laboratory (Document Library), P. O. Box 73, Lexington, Mass 02173
2	IIT Research Institute, ATTN: Dr. Eben Vey, 3422 South Dearborn Street, Chicago 15, Ill
1	IIT Research Institute, ATTN: Dr. T. R. Schiffman, 3422 South Dearborn Street, Chicago 15, Ill
1	MRD Division, General American Transportation Corp., ATTN: G. Nerdhardt, 7501 North Natchez Avenue, Niles, Ill
2	University of New Mexico, ATTN: Dr. Eugene Zwoyer, University Hill, NE, Albuquerque, NM
2	Massachusetts Institute of Technology, Dept of Civil and Sanitary Engineering, ATTN: Dr. Robert V. Whitman, 77 Massachusetts Ave, Cambridge 39, Mass
2	University of Notre Dame, Dept of Civil Engineering, ATTN: Dr. Harry Saxe, Notre Dame, Ind

DISTRIBUTION (cont'd)

No. cys	
2	Purdue University, Civil Engineering Dept, ATTN: Prof G. A. Leonards, Lafayette, Ind
1	United Research Services, ATTN: Kenneth Kaplan, 1811 Trousdale Drive, Burlingame, Calif
2	South Dakota School of Mines and Technology, ATTN: Edwin H. Oshier, Rapid City, South Dakota
10	Paul Weidlinger, 777 Third Ave, New York, NY 10017
1	Shannon & Wilson, Soil Mechanics & Foundation Engineers, ATTN: Mr. Stanley Wilson, 1105 North 38 Street, Seattle 3, Wash
1	United ElectroDynamics, Inc., ATTN: Mr. Ted Winston, 200 Allendale Road, Pasadena, Calif
2	Stanford Research Institute, ATTN: F. M. Sauer and G. R. Fowles, 333 Ravens Wood, Menlo Park, Calif
1	Iowa State University, Dept of Theoretical and Applied Mechanics, ATTN: Glen Murphy, Ames, Iowa
2	University of Illinois, Dept of Civil Engineering, ATTN: Dr. N. M. Newmark, 111 Talbot Laboratory, Urbana, Ill
1	Princeton University, Dept of Civil Engineering, Princeton, NJ
1	University of Illinois, ATTN: D. U. Deere, 111 Talbot Laboratory, Urbana, Ill
1	St Louis University, Institute of Technology, ATTN: Dr. Carl Kisslinger, 3621 Olive St, St Louis 8, Mo
1	Dept of Civil Engineering, ATTN: Frank E. Richardt, Gainesville, Fla
1	University of California, College of Engineering, ATTN: Prof Martin Duke, Los Angeles, Calif
1	Portland Cement Assoc., ATTN: Eivind Hognestad, Manager, Structural Dev. Section, 33 West Grand Ave., Chicago, Ill
1	University of Illinois, ATTN: Prof C. E. Bowman, 111 Talbot Laboratory, Urbanz, Ill
1	National Engineering Science Co., ATTN: Lars Skjelbreia, 711 South Fairoaks Ave, Pasadena, Calif
1	University of Washington, ATTN: Dr. I. M. Fyfe, Seattle 5, Wash
1	West Virginia University, Dept of Civil Engineering, ATTN: Dr James H. Schaub, Morgantown, WVa
1	Northrop-Ventura, ATTN: Dr. J. G. Trulio, 1515 Rancho Conejo, Newbury Park, Calif
1	Physics International, ATTN: Dr. C. S. Godfrey, 2229 Fourth St, Berkeley, Calif

DISTRIBUTION (cont'd)

No. cys	
1	The Boeing Company, Suite 802, First National Bank Bldg, Albuquerque, NM
1	Official Record Copy (Lt Higgins, WLDC)